The quasar main sequence and its potential for cosmology

Paola Marziani[1]

with the "extreme team"

A. del Olmo[2], D. Dultzin[3], J. A. de Diego[3], A. Negrete[3], J. W. Sulentic[2], E. Bon[4], N. Bon[4], M.L. Martínez-Aldama[5], G. M. Stirpe[6], M. D'Onofrio[7], J. Perea[3]

[1] *INAF - Osservatorio Astronomico di Padova, Padova, Italia*

[2] *Instituto de Astrofísica de Andalucía (CSIC), Granada, España*

[3] *Astronomical Observatory, Belgrade, Serbia*

[4] *Instituto de Astronomía, UNAM, México, D.F., México*

[5] *Center for Theoretical Physics, Polish Academic of Sciences, Warsaw, Poland*

[6] *INAF - Osservatorio Astrofísica e Science dello Spazio, Bologna, Italia*

[7] *Dipartimento di Fisica ed Astronomia "Galileo Galilei", U. di Padova, Padova, Italia*

Sept. 23, 2019 Guilin, PRChina

The main sequence (MS) for type-1 (unobscured) quasars

An extreme of the MS:
strongest FeII emitters (i.e., highly accreting quasars)

“Eddington standard candles”?

A main sequence for quasars: preamble

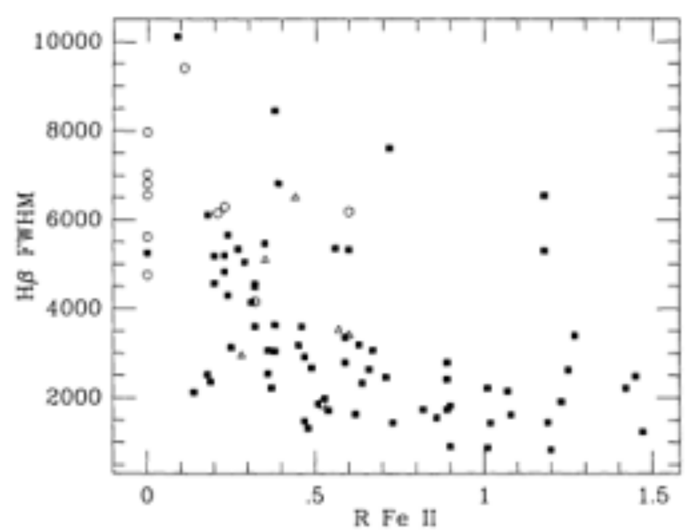

FIG. 9.—FWHM of the Hβ line plotted against R Fe II, the ratio of the equivalent width of the Fe II complex between λ4434 and λ4684 to that of Hβ.

Eigenvector 1 (E1): originally defined by a Principal Component Analysis of parameters measured on the optical spectra of ~80 PG quasars

Boroson & Green 1992

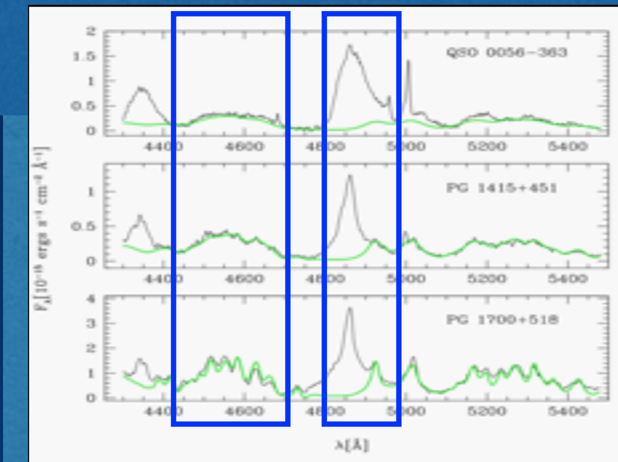

$$R_{\rm FeII} = \frac{I({\rm FeII}\lambda4570)}{I(H\beta)} \approx \frac{W({\rm FeII}\lambda4570)}{W(H\beta)}$$

FeII emission is self-similar but intensity with respect to Hβ changes from object to object

FeII emission from UV to the IR can dominate the thermal balance of the low-ionization BLR

Marinello et al. 2018

E1 main sequence (MS) first associated with an anti-correlation between strength of FeIIλ4570 and width of Hβ (or the peak intensity of [OIII] 4959,5007

Sulentic et al. 2000 [ARA&A], 2002; n ~ 200

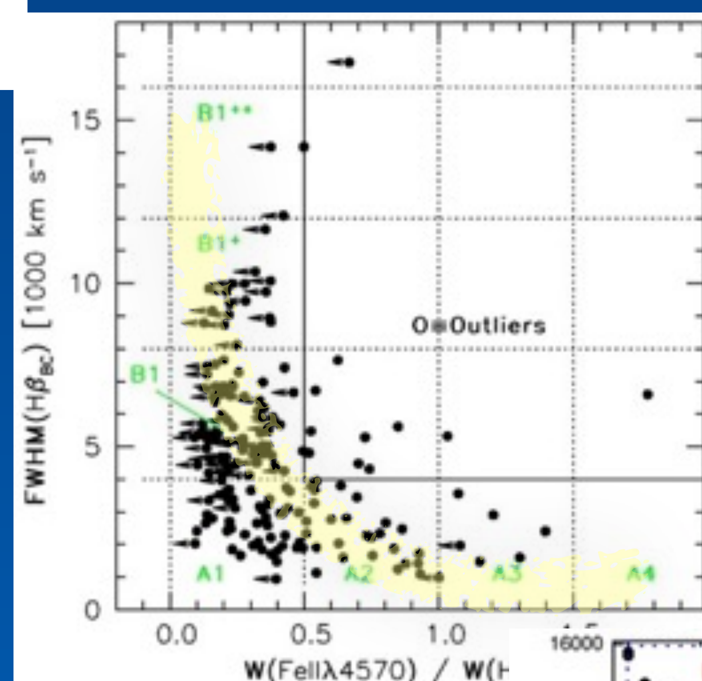

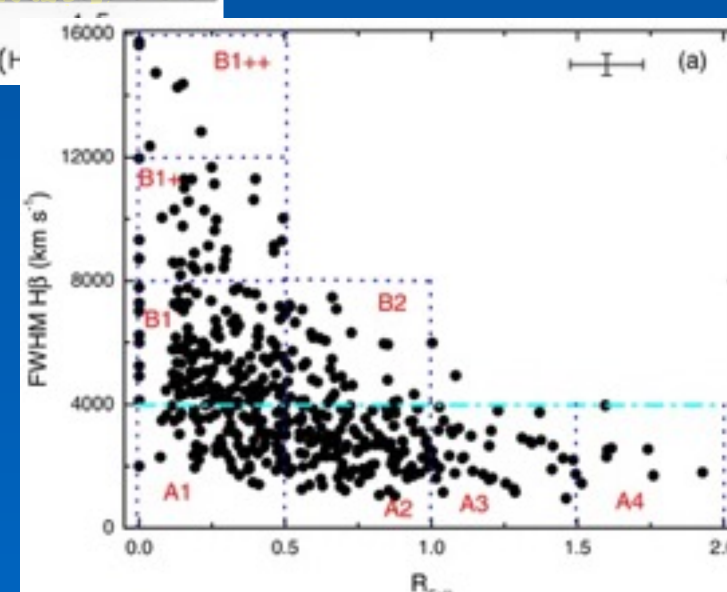

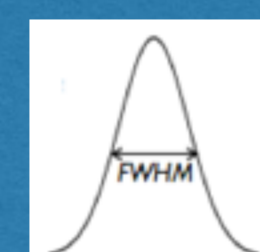

Since 1992, the E1 MS has been found in increasingly larger samples

Zamfir et al. 2010, n ~ 500

FWHM(Hβ): related to the velocity field in the low-ionization BLR (predominantly virialized)

Peterson & Wandel 2000; recent reverberation studies

The main sequence — Organizing quasar diversity

Quasar spectra show a wide range of line profiles, R_{FeII}, line shifts, line intensities ➜ differences in BLR dynamical conditions and ionization levels

Sulentic et all. 2000

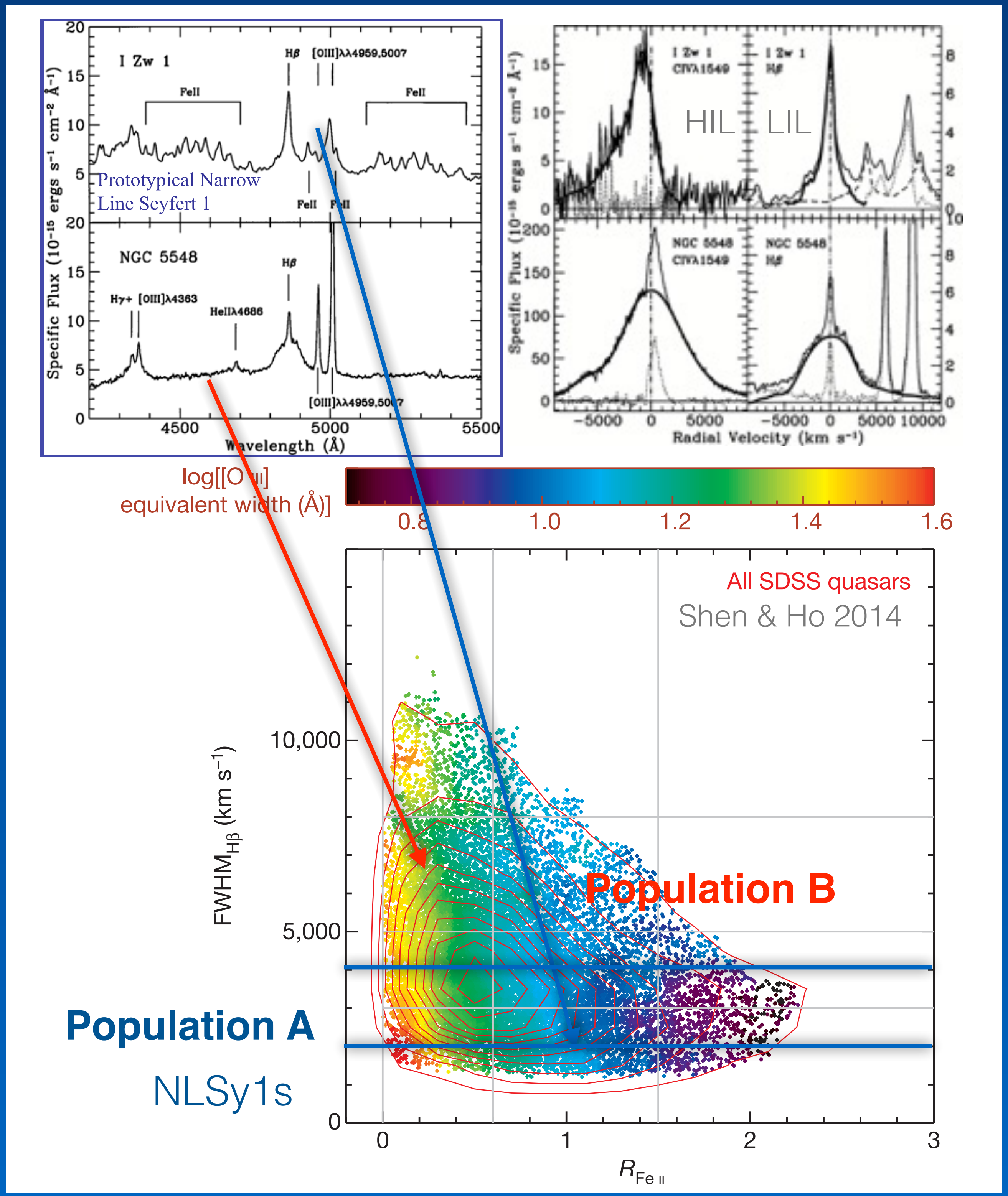

Fraix-Burnet et al. 2017

Key multifrequency parameters related to the accretion process and the accompanying outflows show a trend along the MS

Parameter	Population A	Population B	References
FWHM(Hβ_{BC})	800–4000 km s^{-1}	4,000–10,000 km s^{-1}	1, 2, 3, 4
R_{Fe}	0.7	0.3	1, 2
$c(\frac{1}{2})$ CIVλ1549$_{BC}$	−800 km s^{-1}	−250/+70 (RQ/RL)	5, 6, 7, 8
Γ_S	Often large (> 2)	Rarely large (≈ 2)	2, 9, 4, 10
W(Hβ_{BC})	~ 80 Å	~ 100 Å	2
Hβ_{BC} profile shape	Lorentzian	Double Gaussian	11, 12, 13
$c(\frac{1}{2})$ Hβ_{BC}	~ zero	+500 km s^{-1}	13
SiIII/CIII]	0.4	0.2	14, 15,16
FWHMCIVλ1549$_{BC}$	(2–6) ·10^3 km s^{-1}	(2–10) ·10^3 km s^{-1}	5, 17
W(CIVλ1549$_{BC}$)	Few Å – ≈ 60 Å	~ 100 Å	4, 6, 7
AI(CIVλ1549$_{BC}$)	−0.1	0.05	5
W([OIIIλ5007)	1–20	20–80	1, 18, 19
v_r([OIIIλ5007)	Negative / 0	~ 0 km s^{-1}	4, 18, 19, 20
FIR color α(60, 25)	0–−1	−1–−2	21
X-ray variability	Extreme/rapid common	Less common	22, 23
Optical variability	Possible	More frequent/higher amplitude	24
Probability radio loud	≈ 3–4%	25%	4, 25
BALs	Extreme BALs	Less extreme BALs	36, 37
log density[1]	≳11	≳9.5	14, 28
log U[1]	−2.0/−1.5	−1.0/−0.5	14, 28
log M_{BH} [$M_\odot$]	6.5–8.5	8.0–9.5	7, 8, 29
L/L_{Edd}	≈ 0.2–1.0	~ 0.01 – ≈ 0.2	1, 4, 7, 29, 30, 31

1: Boroson and Green (1992); 2: Sulentic et al. (2000a); 3: Collin et al. (2006); 4: Shen and Ho (2014); 5: Sulentic et al. (2007); 6: Baskin and Laor (2005); 7: Richards et al. (2011); 8: Sulentic et al. (2016); 9: Wang et al. (1996); 10: Bensch et al. (2015); 11: Véron-Cetty et al. (2001); 12: Sulentic et al. (2002); 13: Marziani et al. (2003b); 14: Marziani et al. (2001); 15: Wills et al. (1999); 16: Bachev et al. (2004); 17: Coatman et al. (2016); 18: Zhang et al. (2011); 19: Marziani et al. (2016a); 20: Zamanov et al. (2002); 21: Wang et al. (2006); 22: Turner et al. (1999); 23: Grupe et al. (2001); 24: Giveon et al. (1999); 25: Zamfir et al. (2008); 26: Reichard et al. (2003); 27: Sulentic et al. (2006); 28: Negrete et al. (2012); 29: Boroson (2002); 30: Peterson et al. (2004); 31: Kuraszkiewicz et al. (2000).

The main sequence — Population A and NLSy1s

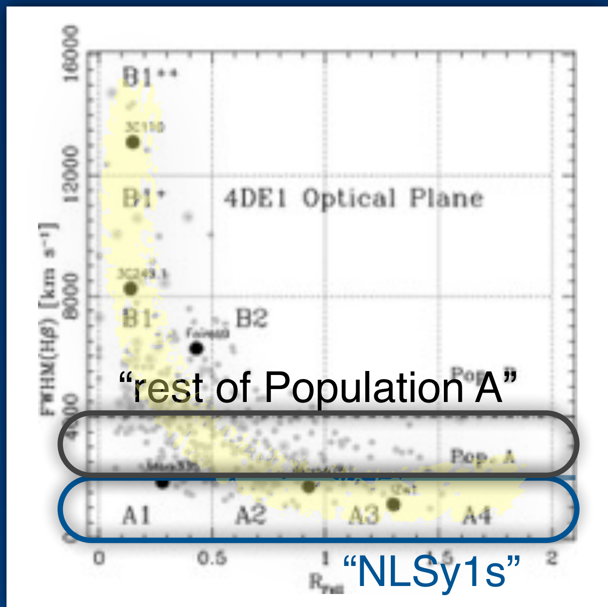

NLy1s (FWHM(Hβ) < 2000 km s^{-1}) vs
“rest of Population A”: 2000 km s^{-1} < FWHM(Hβ) < 4000 km s^{-1}

No change in Hβ shape occurs around FWHM(Hβ) = 2000 km s^{-1}

NLSy1s seamlessly occupy the low-end of the distribution of FWHM(Hβ)

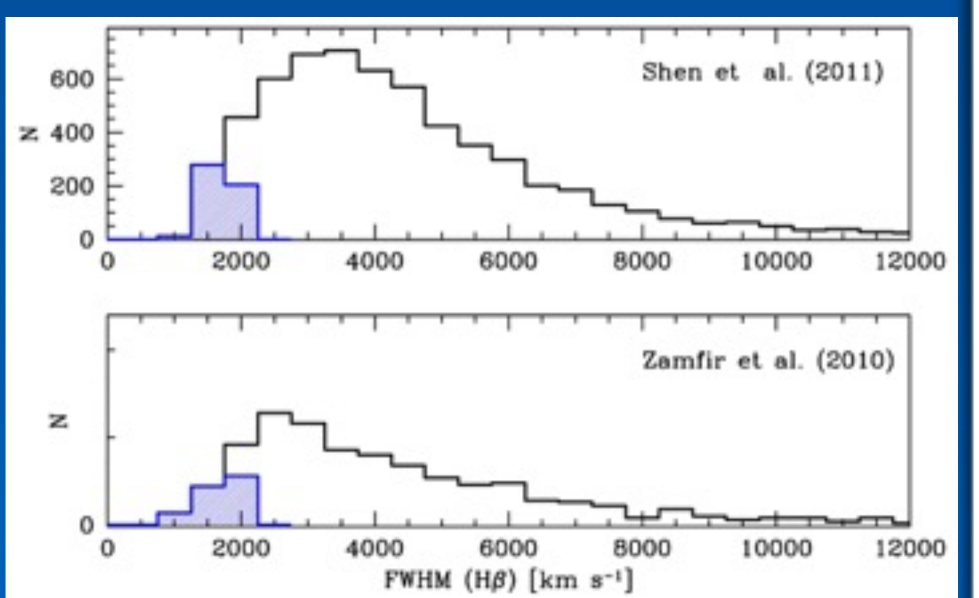

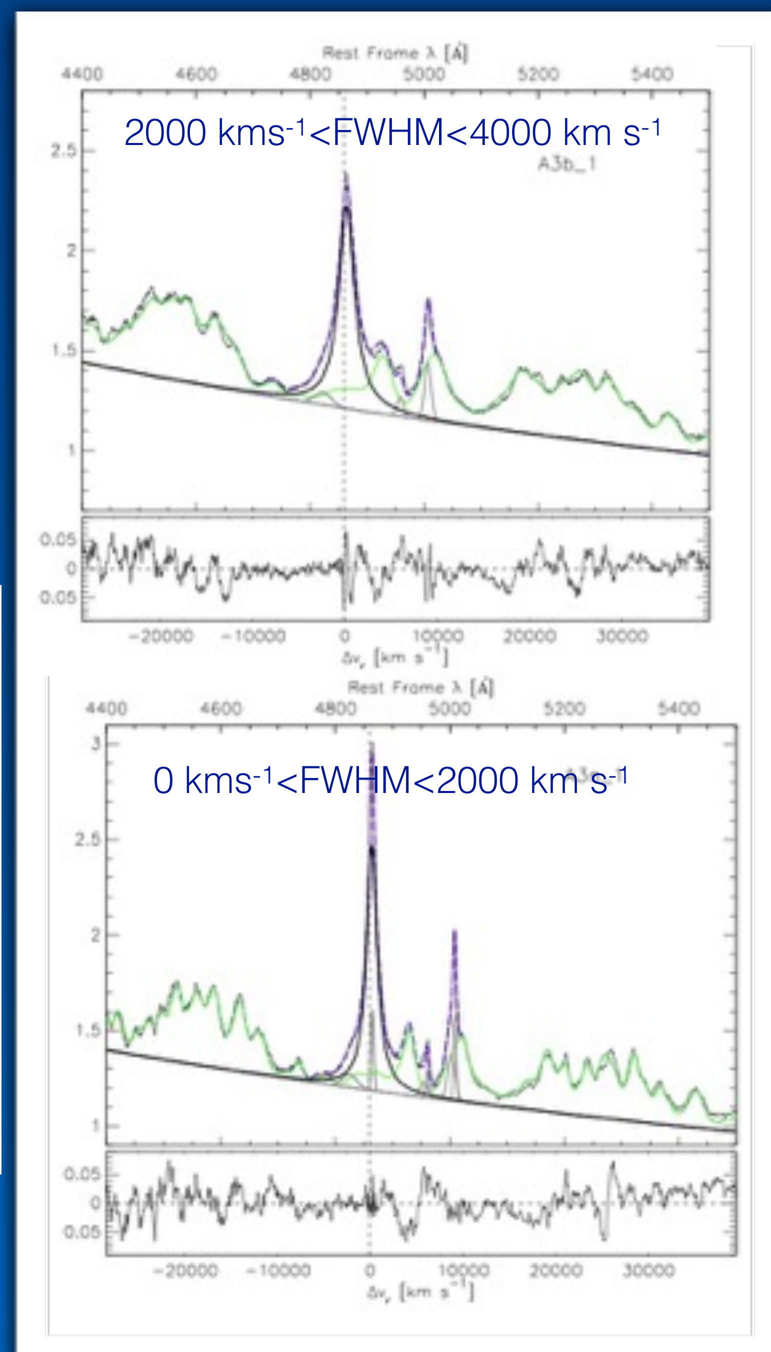

CIV blueshift amplitudes among NLSy1s depend on the spectral type i.e., they increase with R_{FeII}

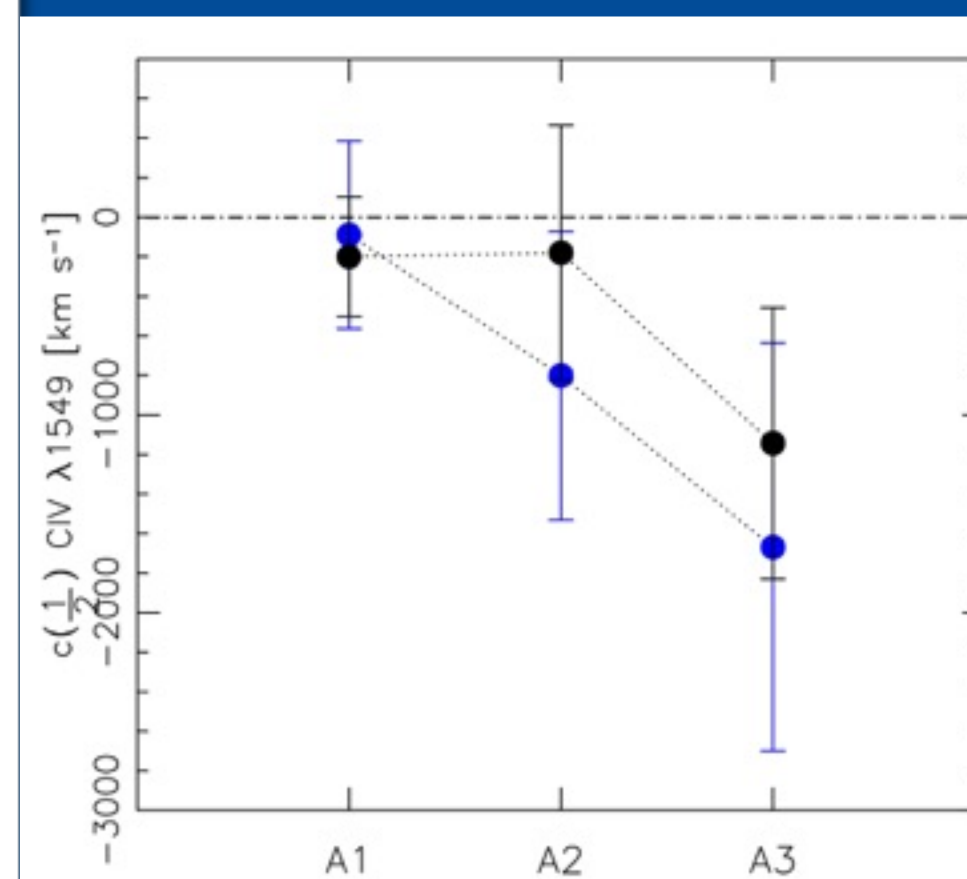

MS correlates — The profiles of Hydrogen Balmer line Hβ

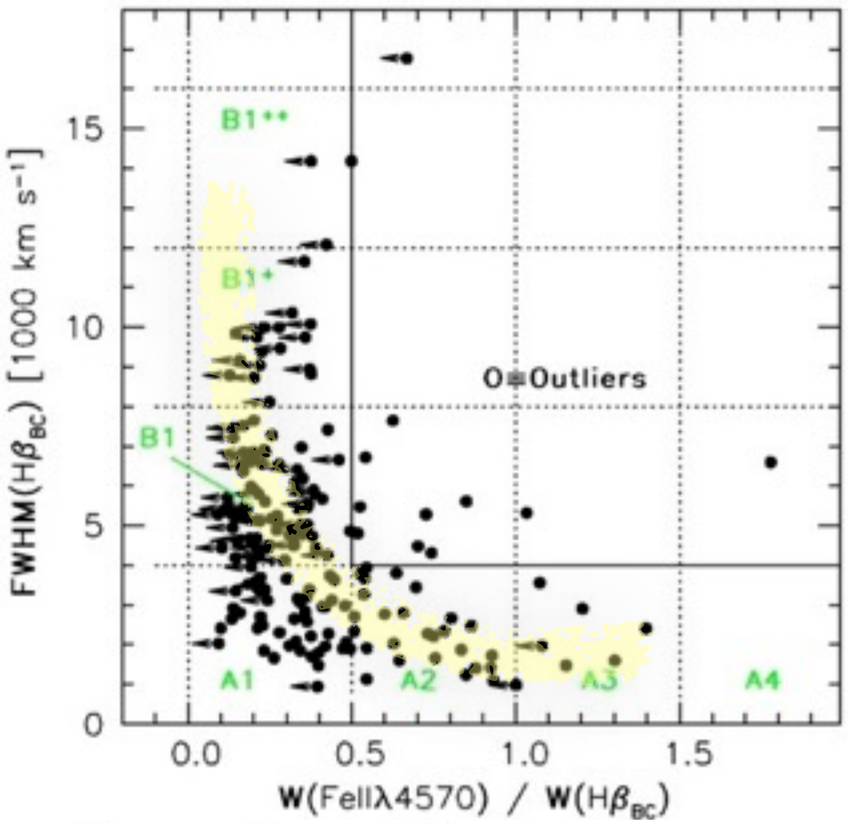

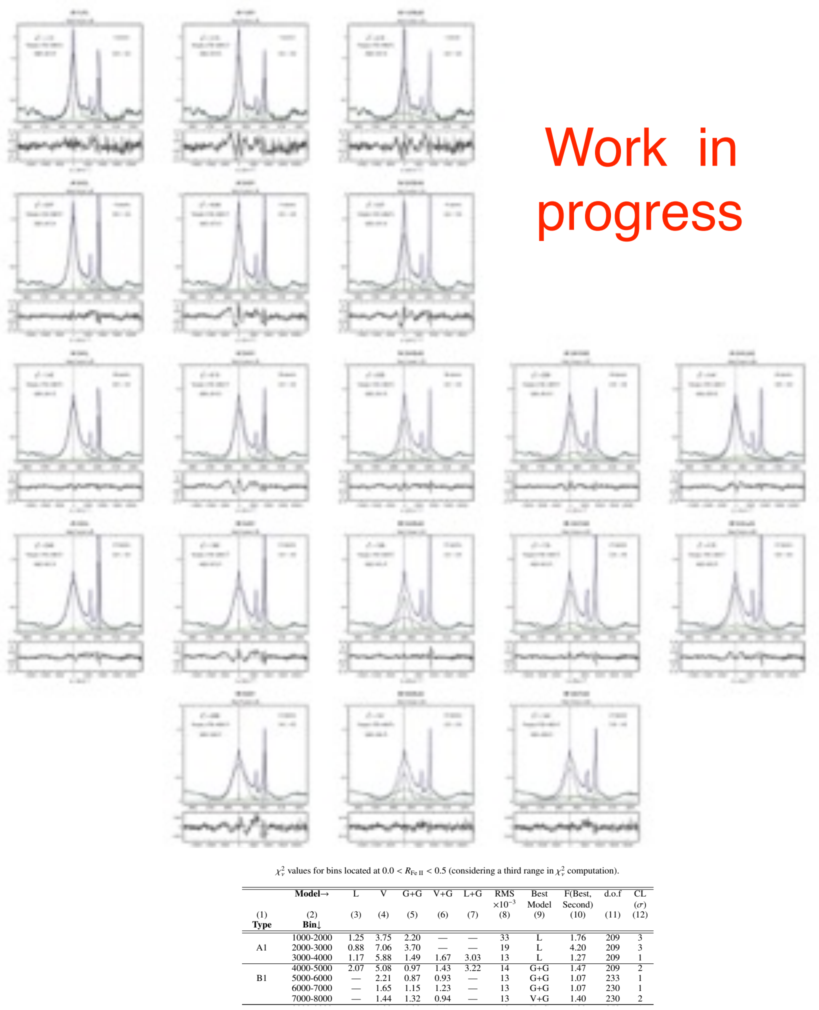

The MS allows for the definition of spectral types

Composite spectra: Pop. A: "Lorentzian" Hβ profile, symmetric, unshifted; Pop. B: Double Gaussian (broad + very broad component Hβ$_{BC}$+Hβ$_{VBC}$), slightly redward asymmetric ➜ predominantly virialized

Fits on composites with several functions (Voigt, single Gaussian, etc.) in steps of 1000 km s^{-1} confirm the Lorentzian as best profile up to 4000 km s^{-1}

Sulentic et al. 2002 (z < 1, log L < 47 [erg/s]); del Olmo et al. in preparation

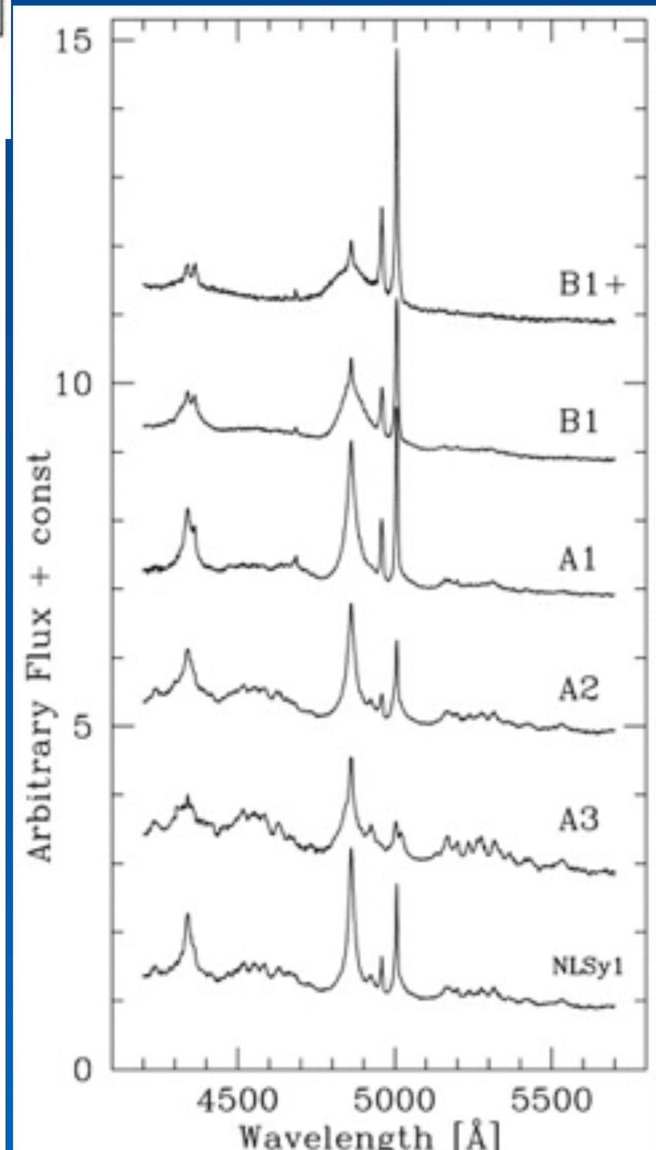

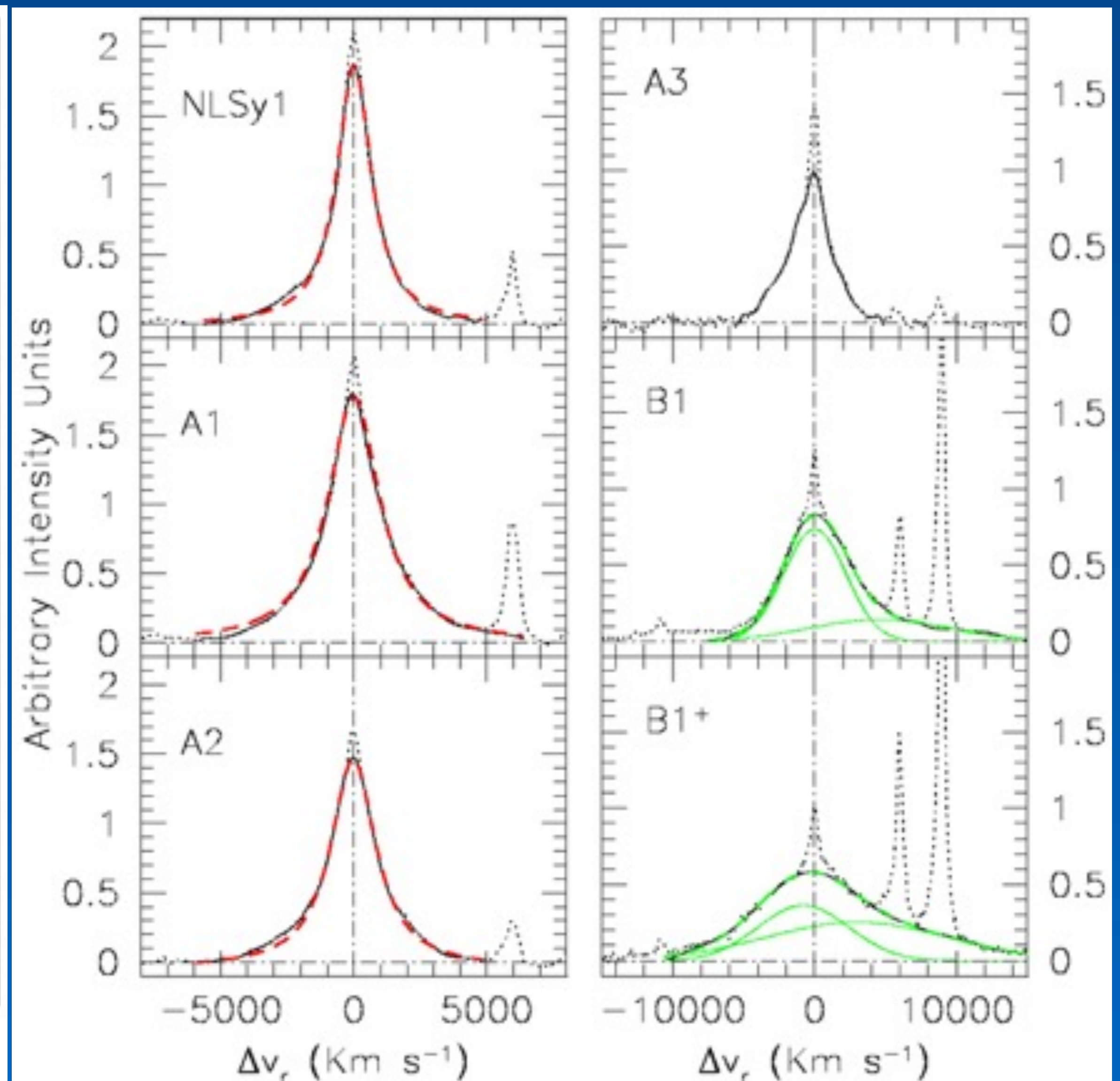

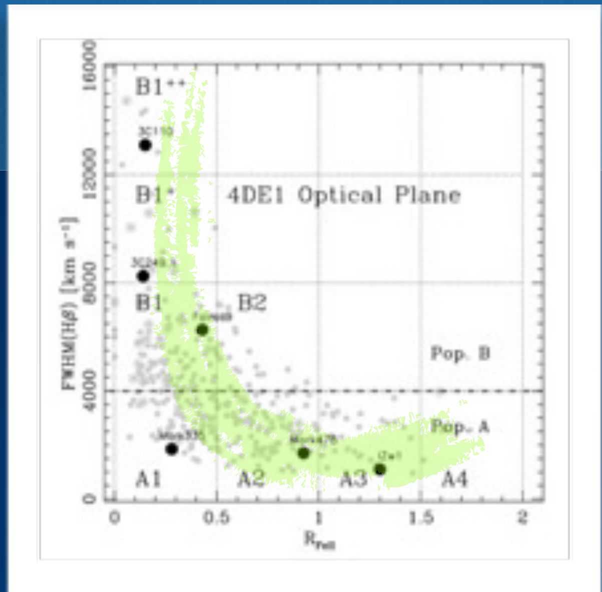

MS correlates — The HIL CIλ1549 profile

The CIVλ1549 line profile: low-ionization "virialized" and high ionization outflow/wind components coexisting even at the highest luminosities

scaled Hβ + excess blueshifted emission

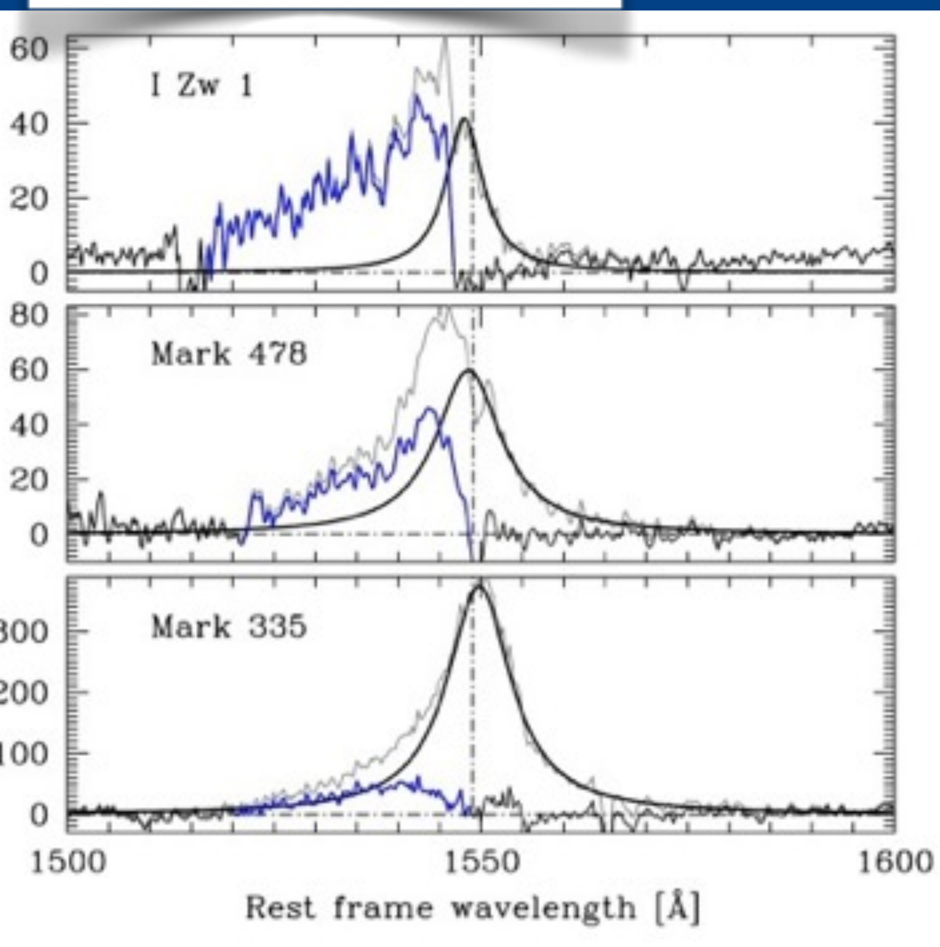

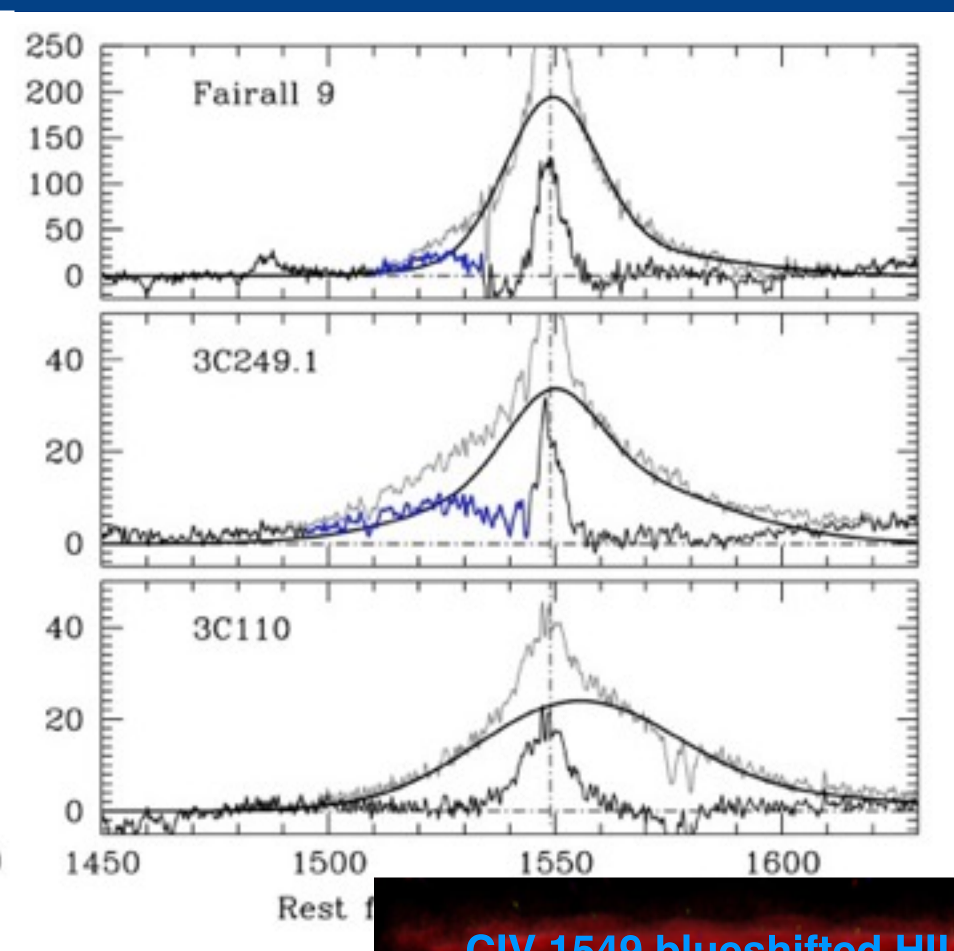

L>10^{47} erg s^{-1}: extremely high amplitude blueshifts in CIV 1549 profiles of Hamburg ESO Pop. A quasars

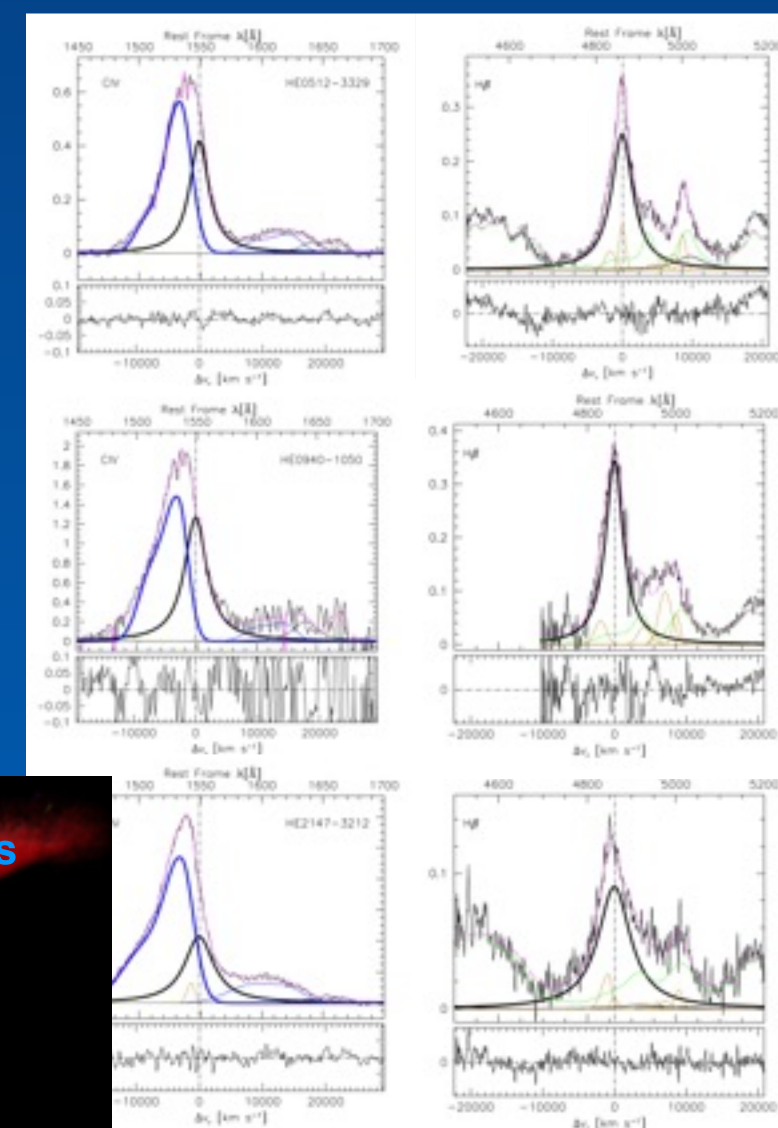

e.g., Leighly 2000, Bachev et al. 2004, Marziani et al. 2010; Denney et al. 2012

A flattened low-ionization sub-system is supported by recent spectropolarimetric results

Popovic et al. 2018; Afanasiev et al. 2019

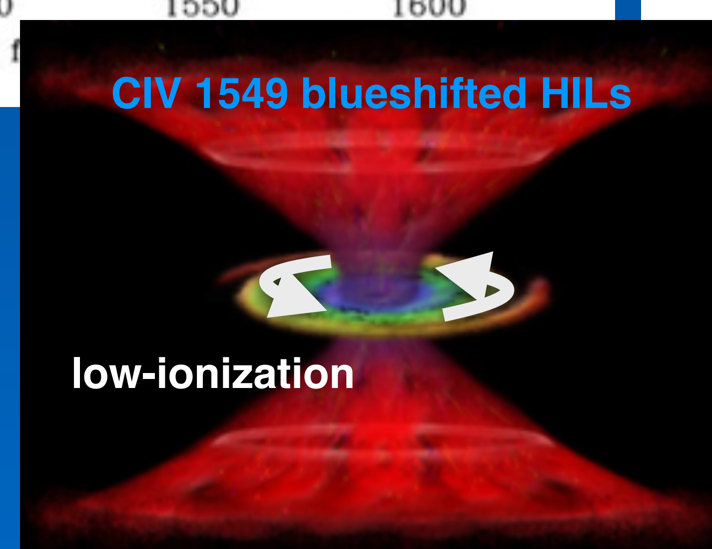

Elvis 2000

MS correlates — UV lines

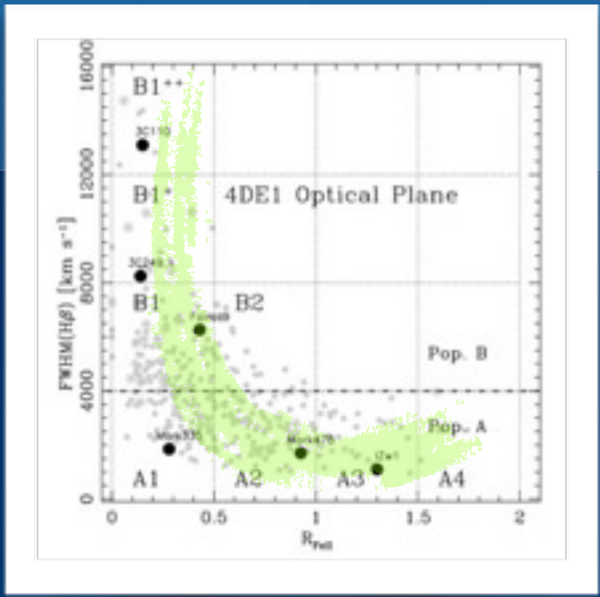

Several trends involving strong UV emission lines

(B1++ → A4) NVλ1240/Lyα⬆ AlIIIλ1860/SiIII]λ1892⬆ CIII]λ1909/SiIII]λ1892⬇ W(NIII]1750) ⬆ W(CIVλ1549) ⬇

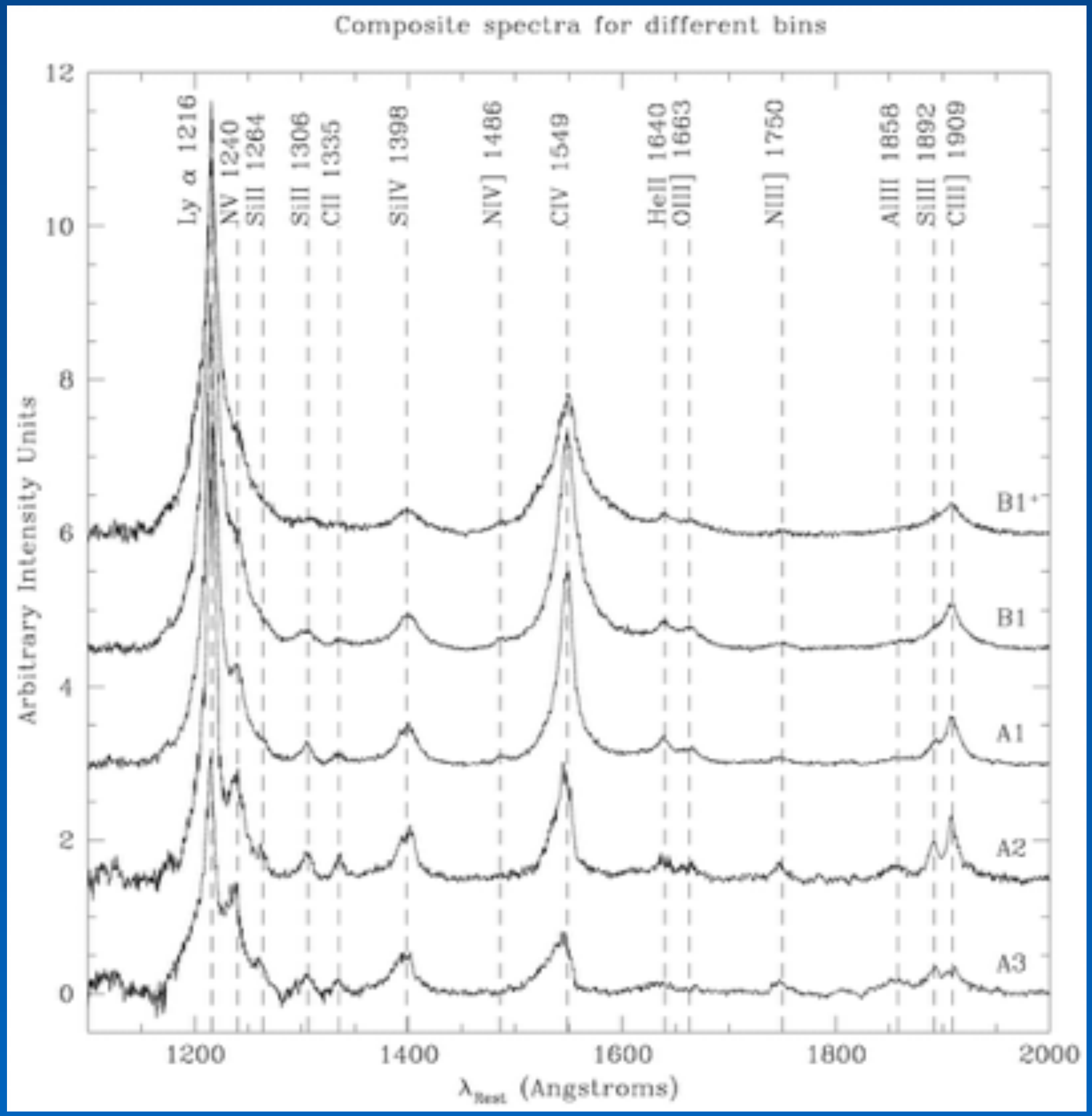

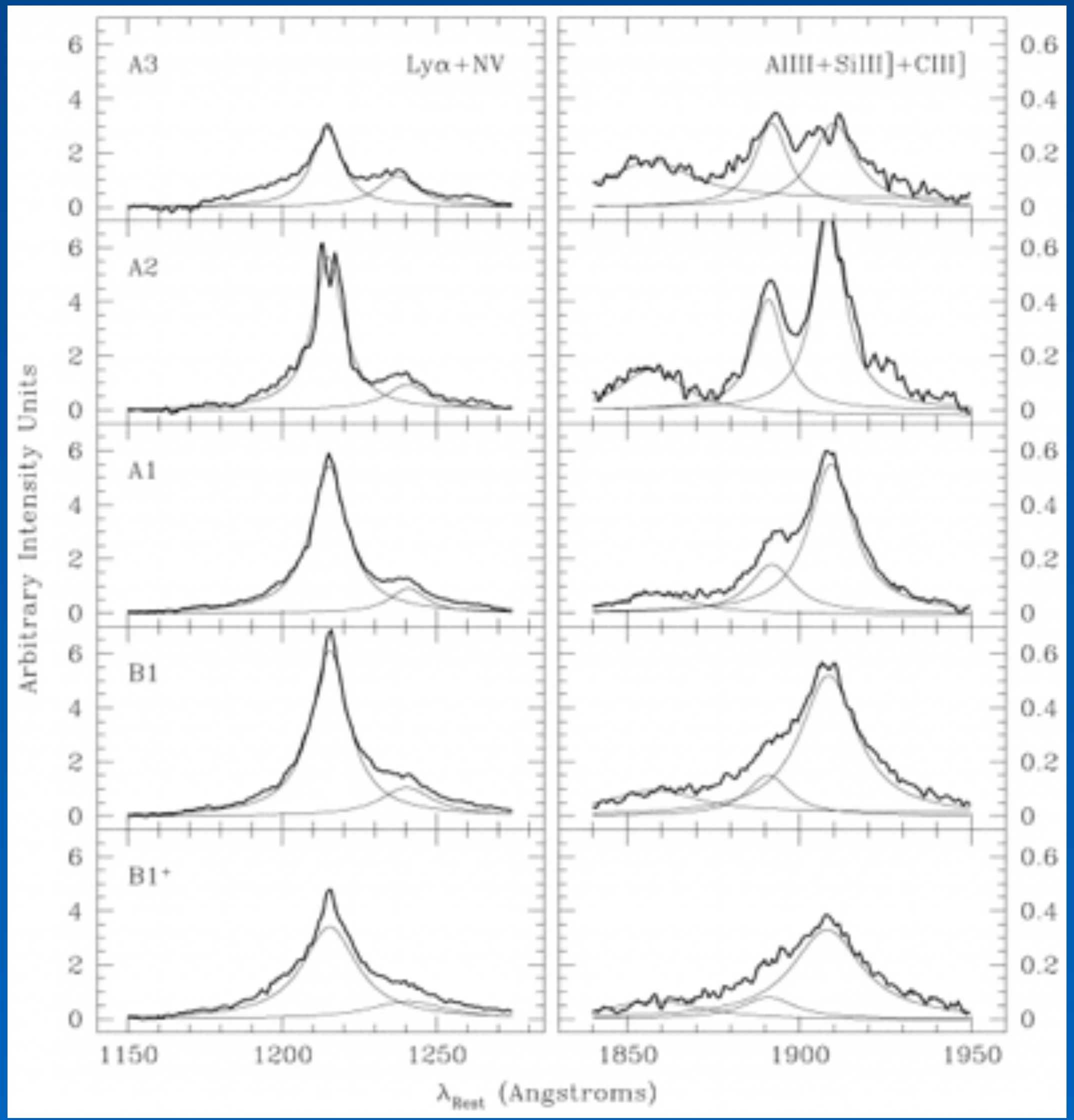

Bachev et al. 2004; HST/FOS composite spectra of quasars at *z*<0.7

MS correlates — L/L_{EDD} as the MS driver

The M_{BH} proxy $\sigma_\star$ increases with R_{FeII} in narrow luminosity bins
$\Rightarrow L/L_{Edd}$ increases with R_{FeII}

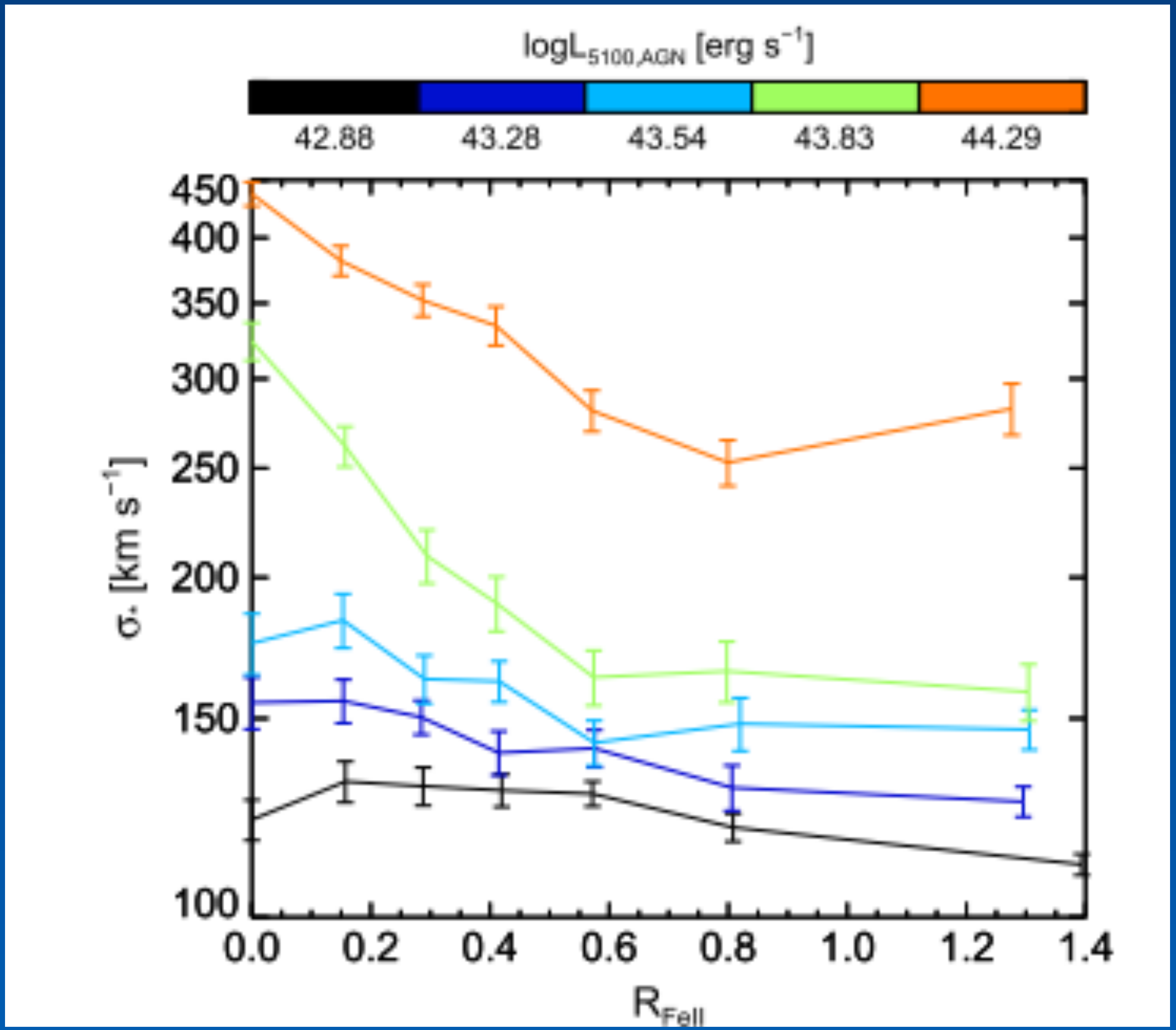

Sun & Shen 2015

Fundamental plane of accreting massive black holes

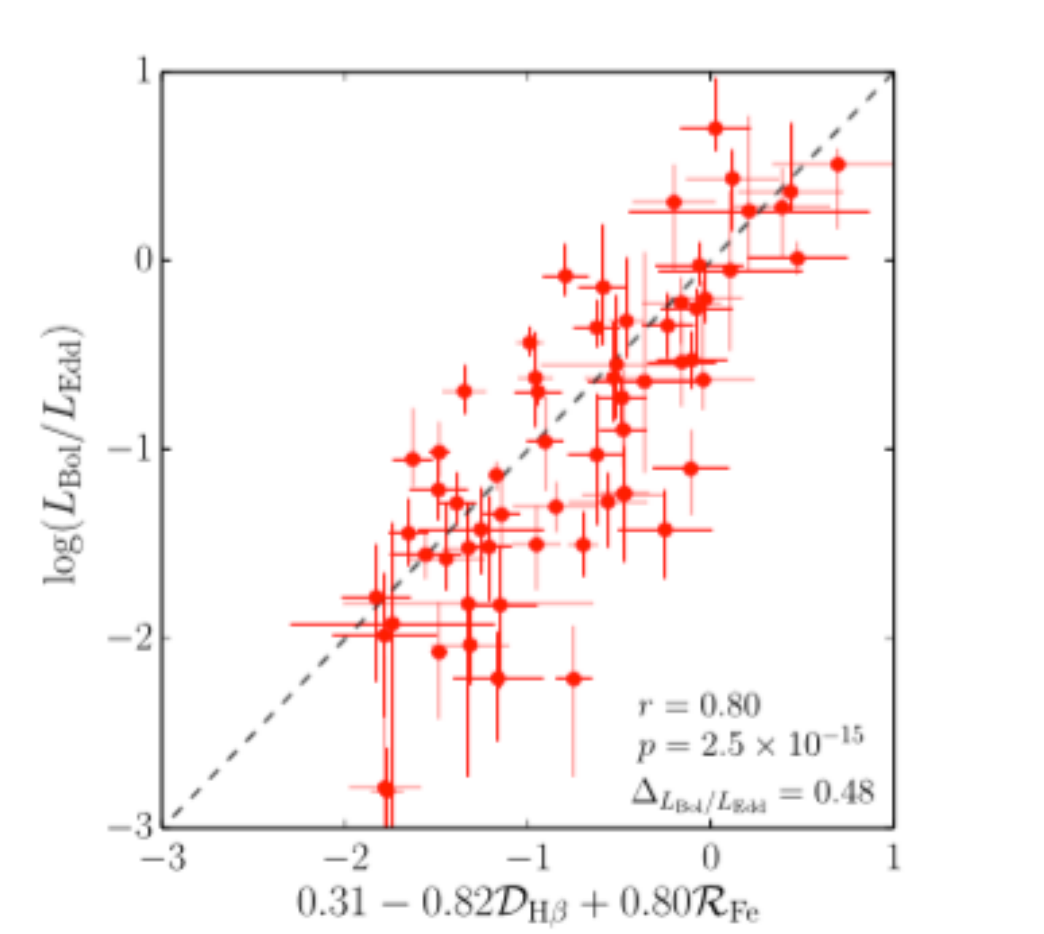

$$\log(\dot{\mathscr{M}}, L_{\rm bol}/L_{\rm Edd}) = \alpha_k + \beta_k \mathcal{D}_{\rm H\beta} + \gamma_k \mathcal{R}_{\rm Fe},$$

$$\mathcal{D}_{\rm H\beta} = \frac{\rm FWHM}{\sigma_{\rm H\beta}},$$

Du et al. 2016, assumed virial relation

Several approaches consistently support a relation between L/L_{Edd} and R_{FeII}

MS correlates — L/L_{EDD} as the MS driver

The optical MS plane at low-z can be understood in terms of Eddington ratio and orientation

(Marziani et al. 2001, 2018; Shen & Ho 2014; Panda et al. 2019)

Population A mainly due to high radiators ($L/L_{Edd} \gtrsim 0.1$-0.2) ;
Pop. A includes rare ($P(\theta) \propto \sin\theta$) lower L/L_{Edd} sources observed almost face-on;
NLSy1s preferentially sample face-on sources;
Degeneracy between mass and viewing angle;
A sharp FWHM limit is not very meaningful.

virial $M_{BH} \Rightarrow$ FWHM $\propto M_{BH}^{1/4} (L/L_{Edd})^{-1/4} f(\theta)^{-1/2}$;

"limb darkening" $\Rightarrow R_{FeII} \propto R_{FeII}(L/L_{Edd}) \cos\theta\, (1 + b \cos\theta)$

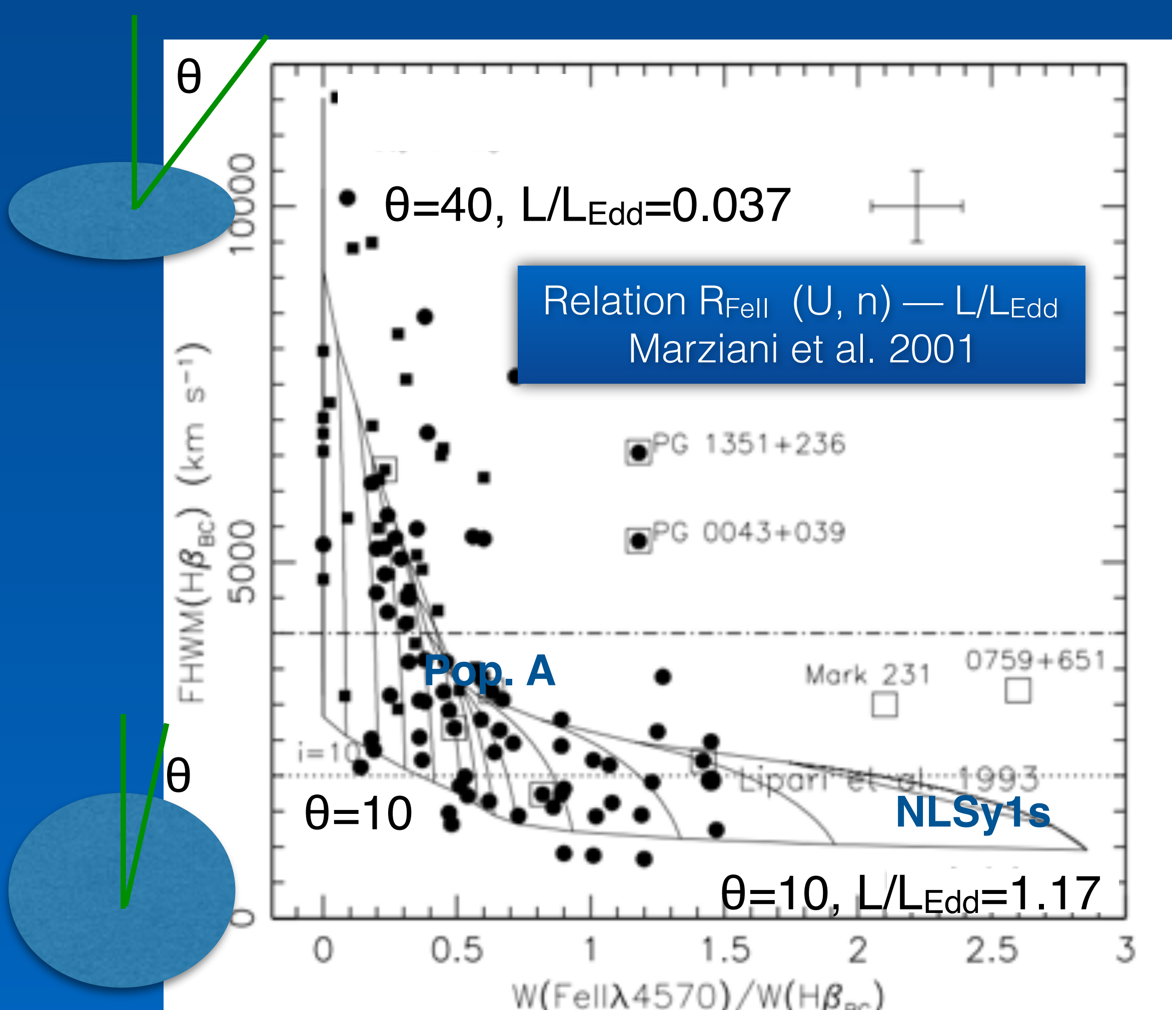

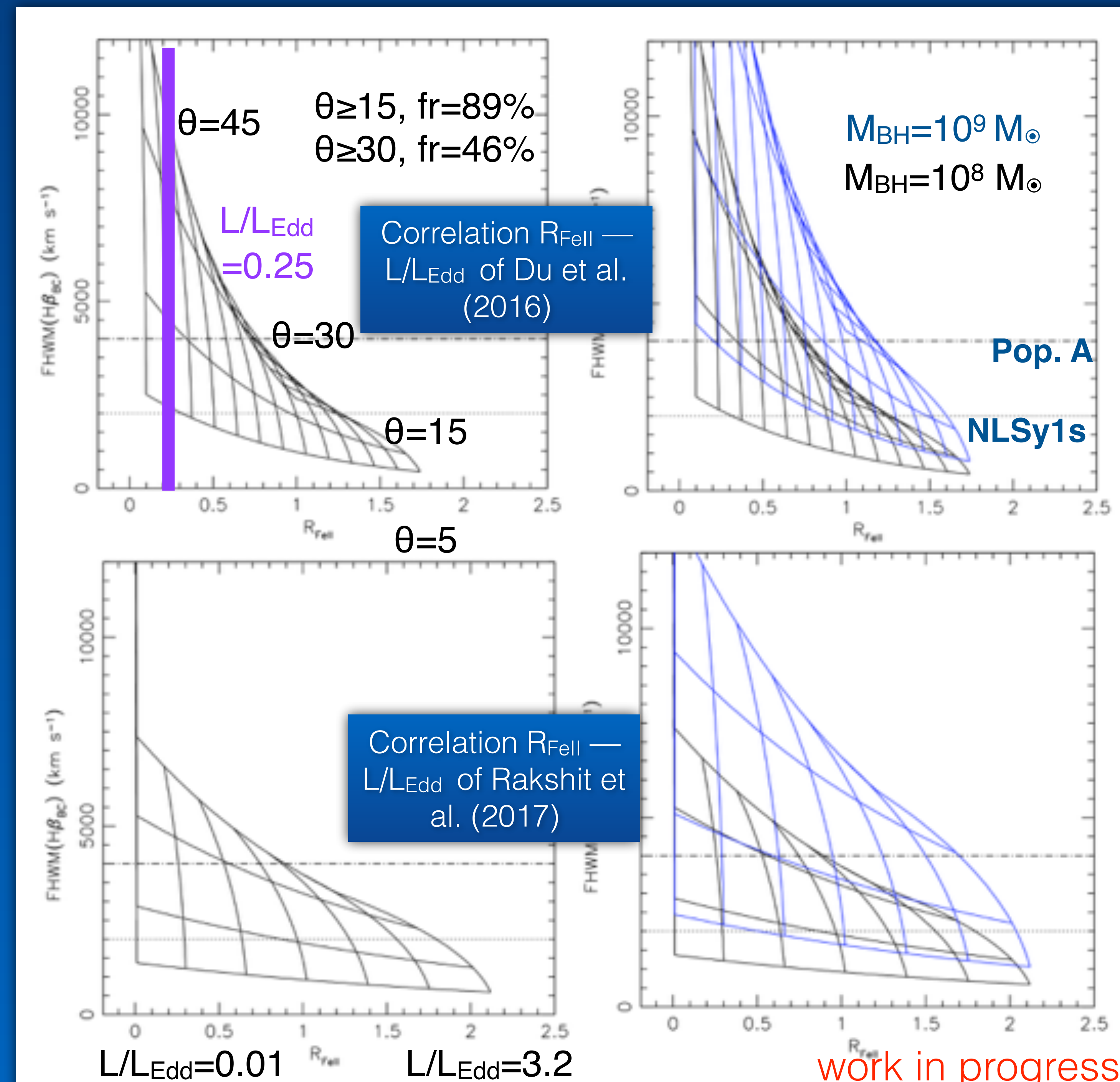

The “high R_{FeII} end” of the quasar MS (extreme Population A, xA, at $R_{\mathrm{Fe}} \gtrsim 1$)

Extreme Population A — Selection and physical conditions

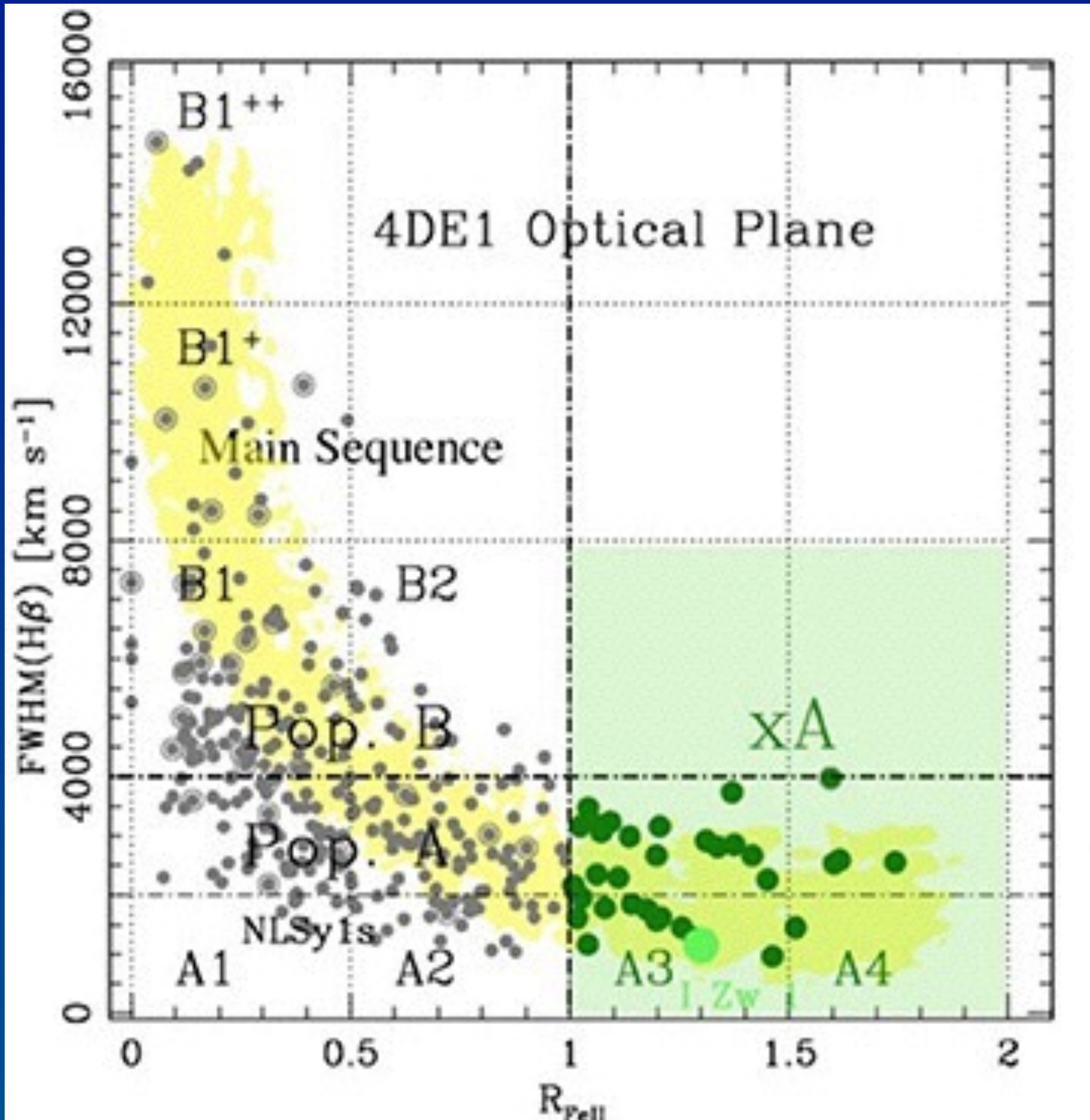

Negrete et al. 2018

Extreme Population A (xA) quasars satisfy $R_{FeII} > 1$; ~ 10% of quasars in low-z, optically selected samples

xA spectra show distinctively strong FeII emission and Lorentzian Balmer line profiles

xAs are related to Super-Eddington accreting massive black holes (SEAMBHs)

Wang et al. 2013; 2014; Du et al. 2016

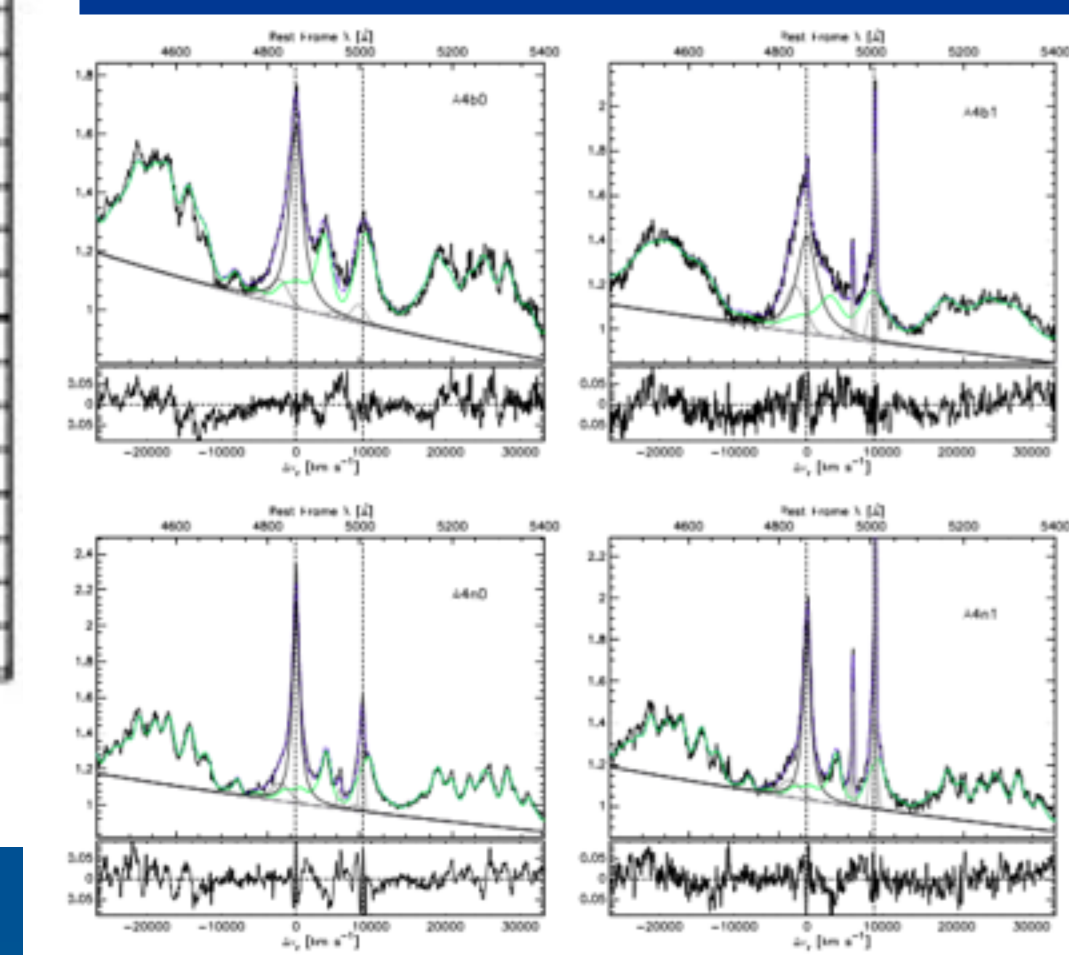

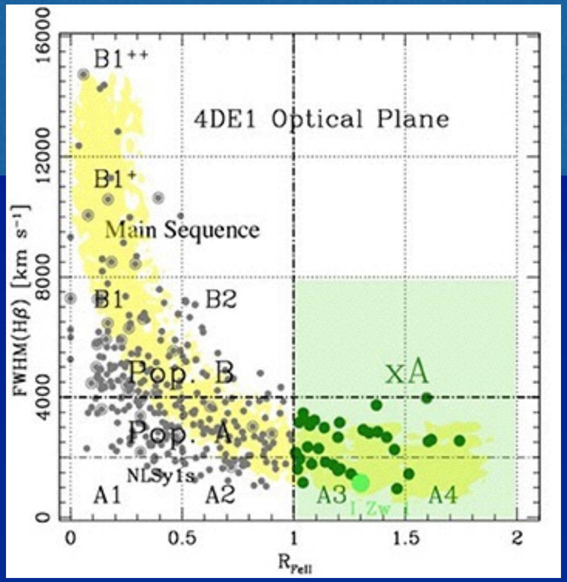

Extreme Population A — Selection and physical conditions

The UV spectrum of xA quasars at z ~ 2

Symmetric low-ionization and blueshifed high-ionization lines even at extreme radiative output

Lines have low equivalent width: some xAs are weak lined quasars

CIII] almost disappears

Martínez-Aldama et al. 2018, and reference therein

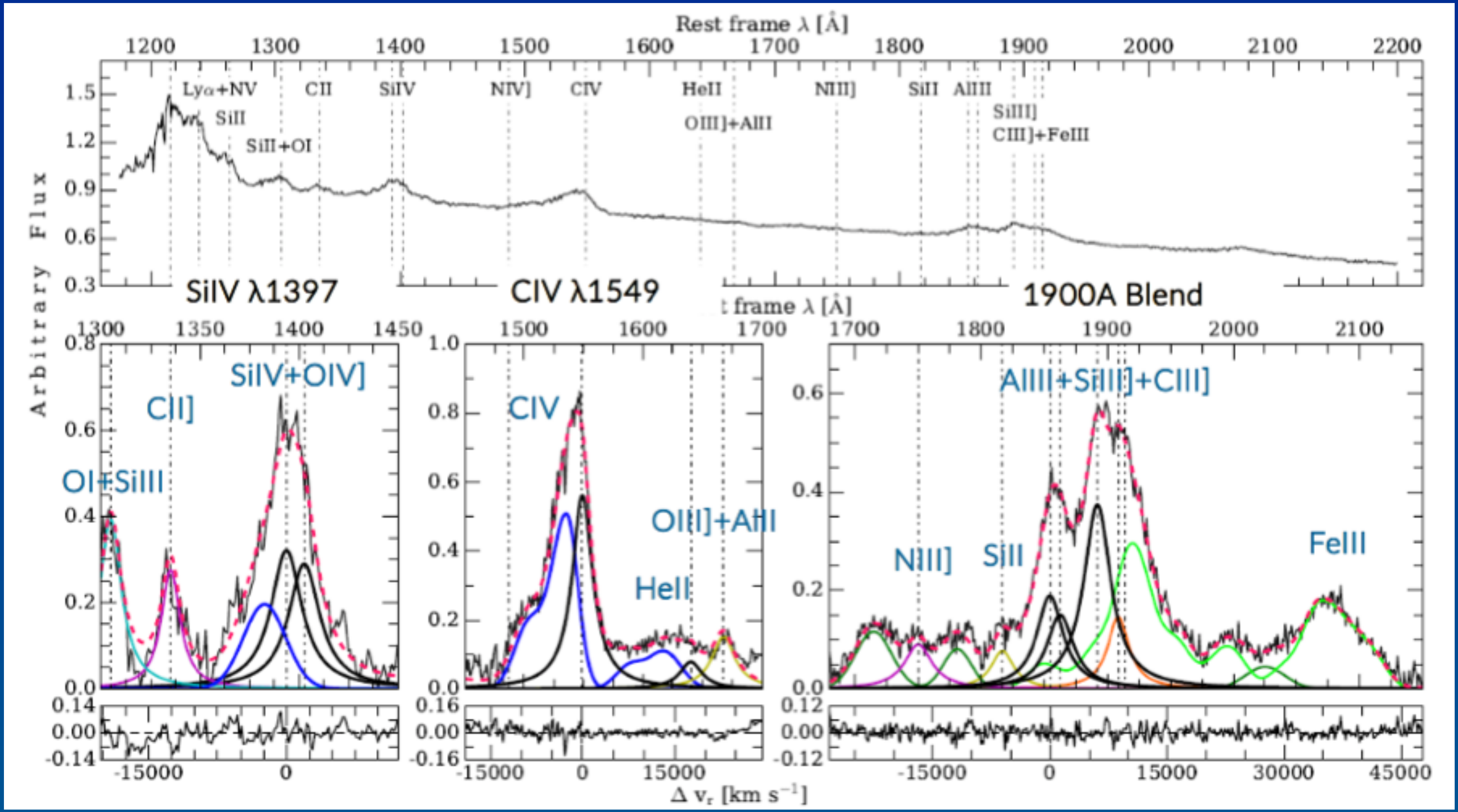

Extreme Population A — Selection and physical conditions

At least 70%-80% of weak-lined quasars [W(CIVλ1549) ≦10 Å] belong to extreme Pop. A

WLQs and xA show continuity in CIV shifts and equivalent widths

WLQs appear as extremes of extreme Population A

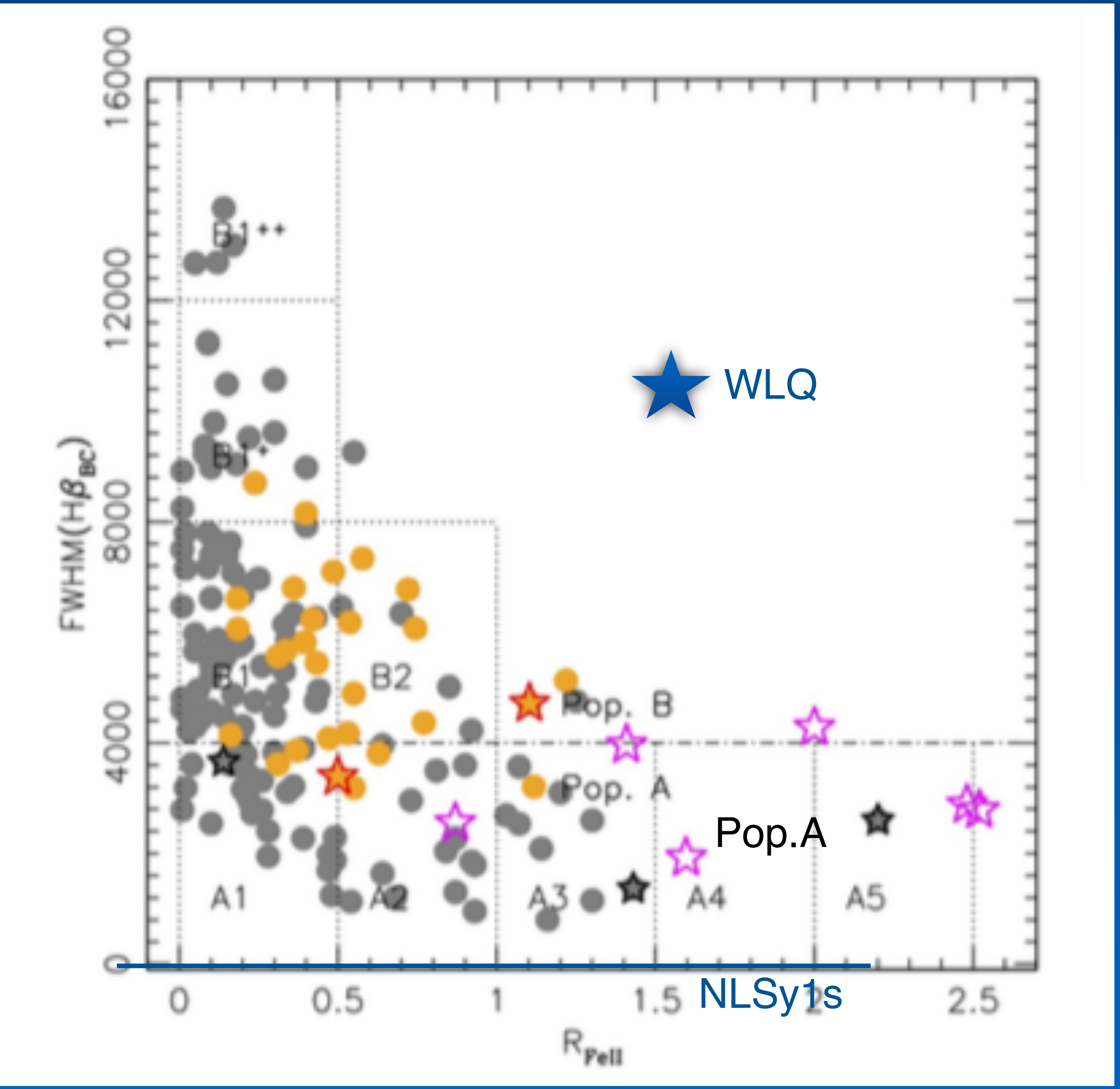

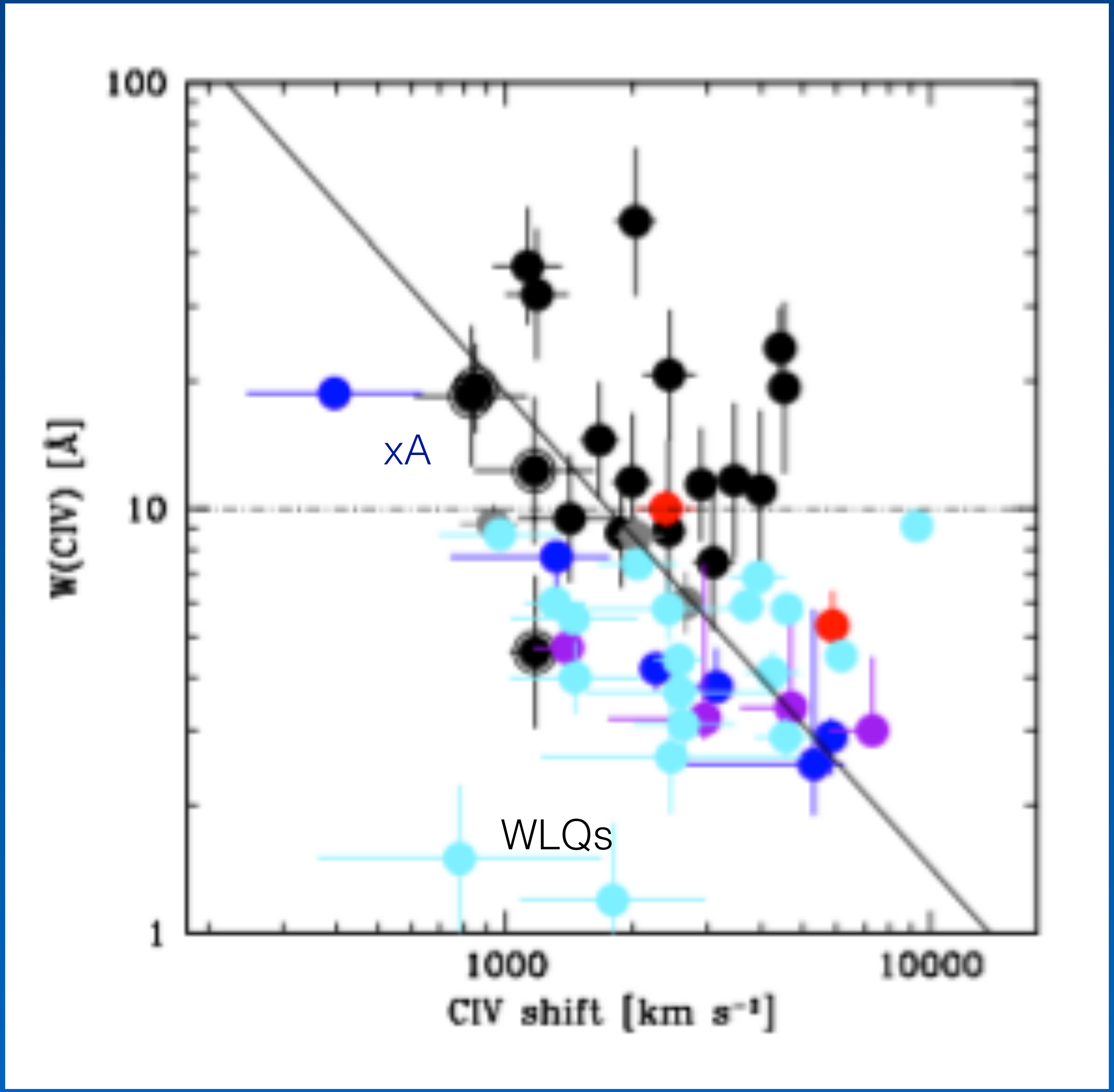

Data from Plotkin et al. 2015; Luo et al. 2015, Wu et al. 2012; Marziani et al. 2016; GTC xA: Martinez-Aldama et al. 2018,

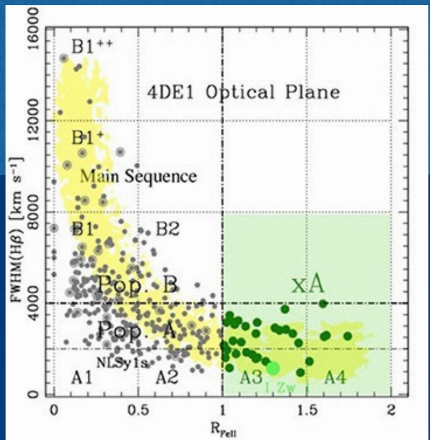

Extreme Population A — Selection and physical conditions

Selection criteria from diagnostic line ratios
1) R_{FeII} = FeIIλ4570 blend/Hβ > 1.0
2) UV AlIII λ1860/SiIII]λ1892>0.5 &
SiIII]λ1892/ CIII]λ1909>1

Extreme Pop. A (xA; R_{FeII}>1):
consistent line intensity ratios (even at
FWHM > 4000 km s^{-1} at high L
for virialized (Balmer and Paschen lines).

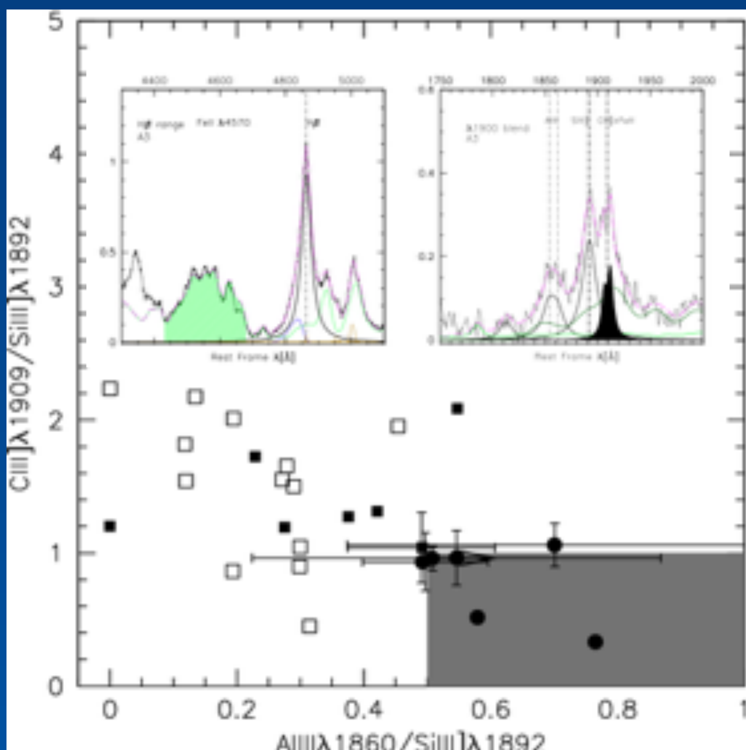

UV and optical selection criteria are equivalent

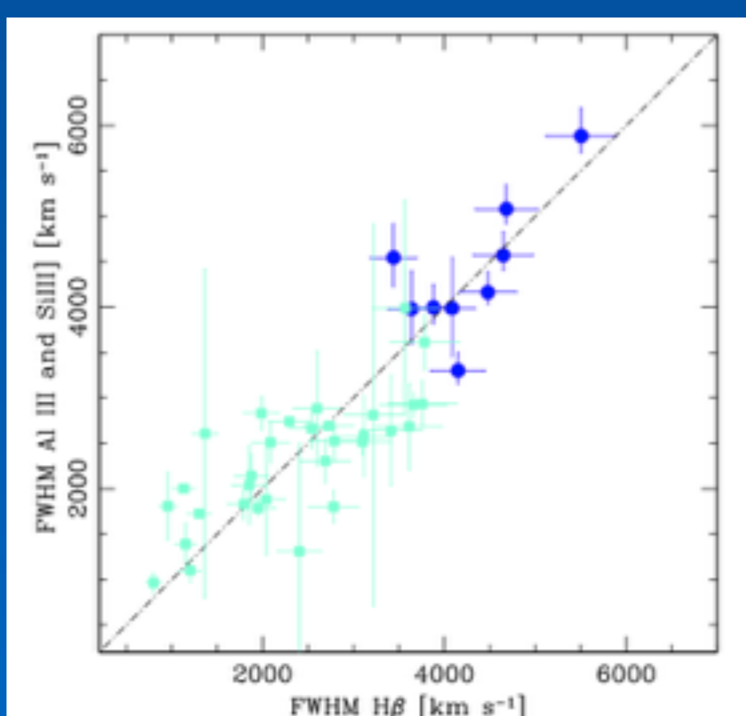

FWHM(Hβ) ~ FWHM(AlIII 1860)
AlIII 1860 virial broadening estimator equivalent to Hβ

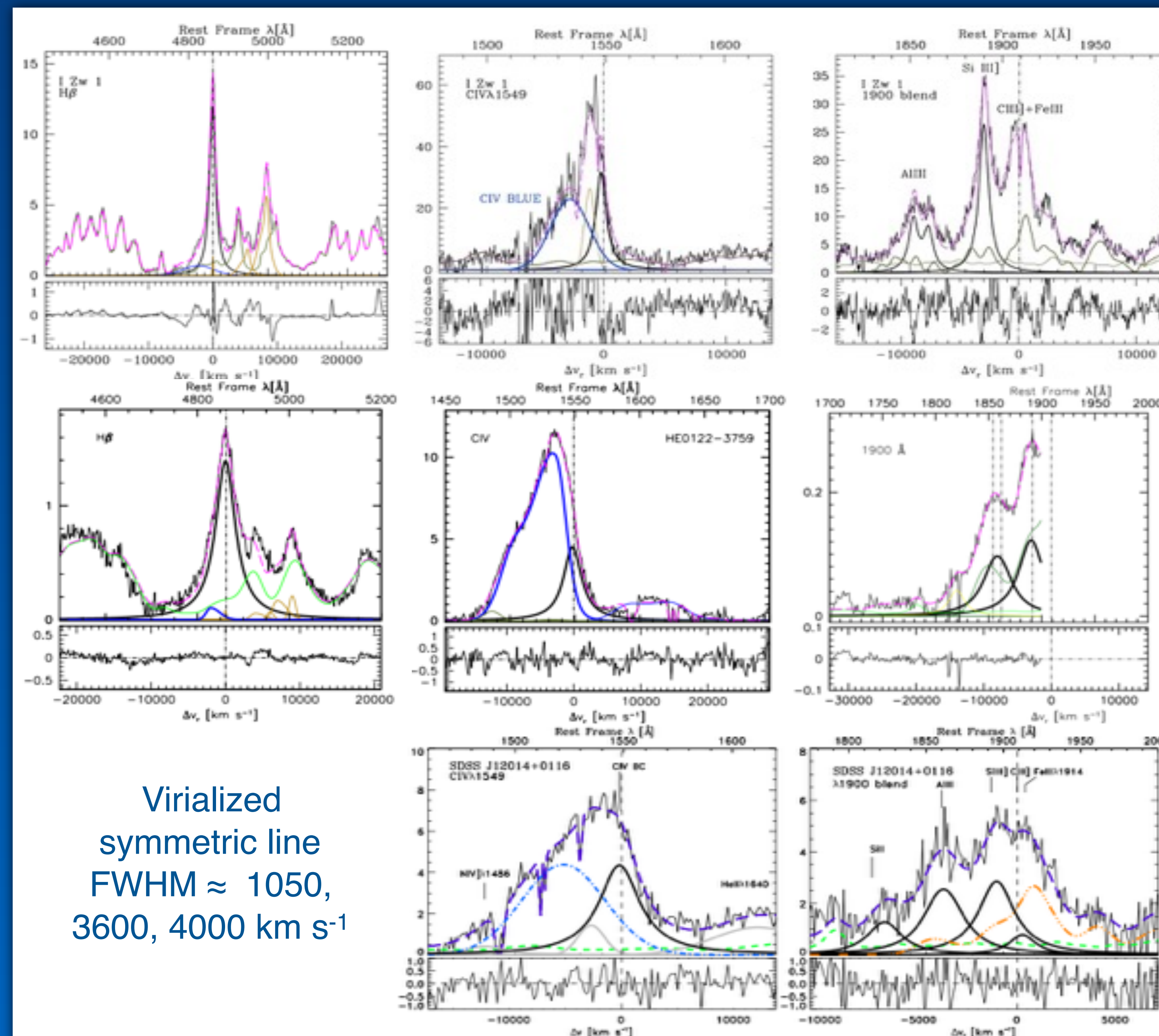

Virialized symmetric line FWHM ≈ 1050, 3600, 4000 km s^{-1}

Extreme Population A — Selection and physical conditions

Extreme values for density (high, $n > 10^{12}$-10^{13} cm^{-3}),
ionization (low, $U \sim 10^{-3}$-$10^{-2.5}$);
radiation forces removed low-density gas?

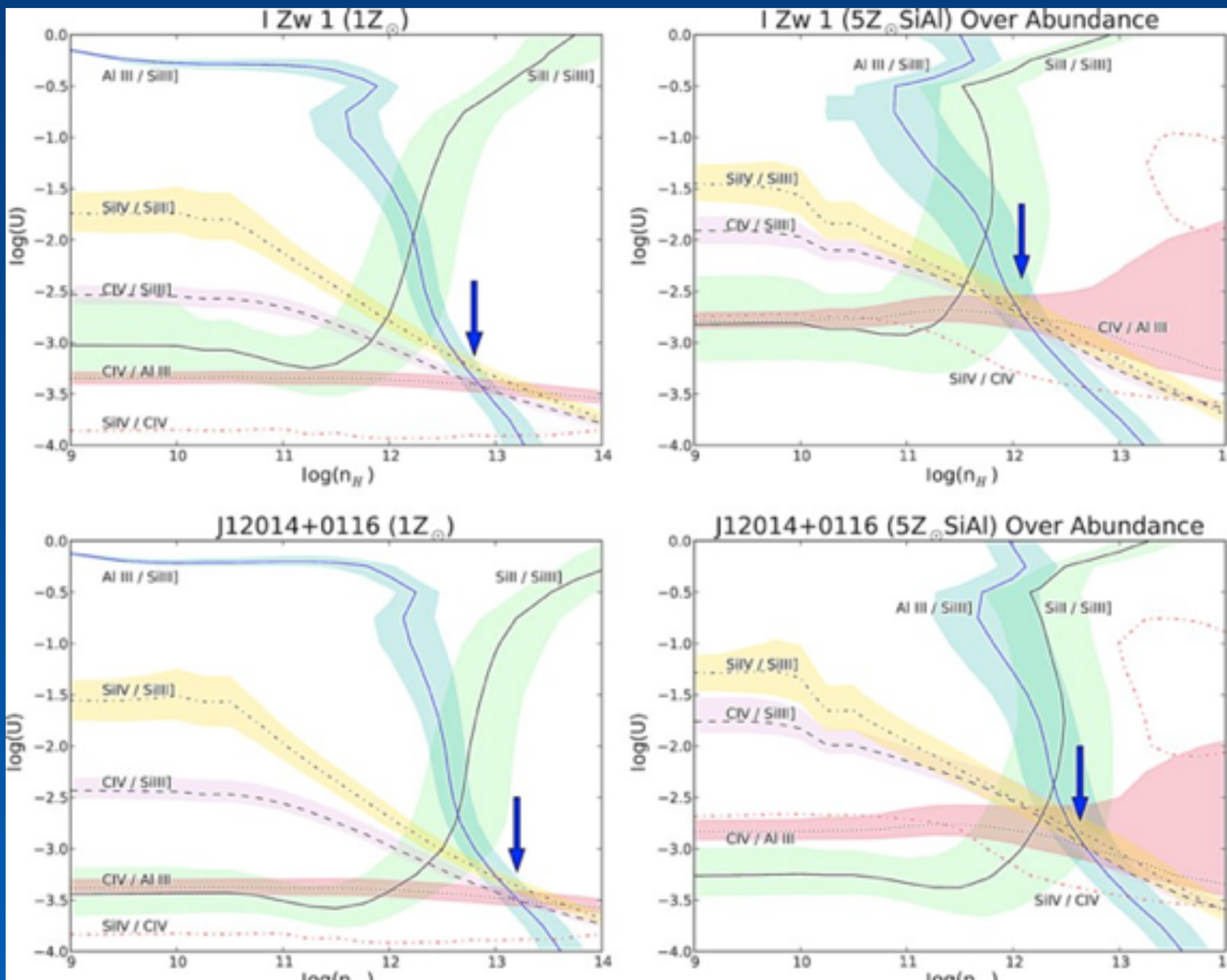

Plane ionization parameter versus density from arrays of CLOUDY simulations

(Negrete et al. 2012; Martínez-Aldama et al. 2018;
Sniegowska et al. 2019 in preparation;
D'Onofrio & Marziani 2018)

Work in progress: Extreme values of metallicity ($Z > 20\ Z_\odot$) or peculiar metallicity with anomalies in Al

xA sources enriched by a circumnuclear Starburst

xA sources: the "first" unobscured stage emerging from an obscured evolution?

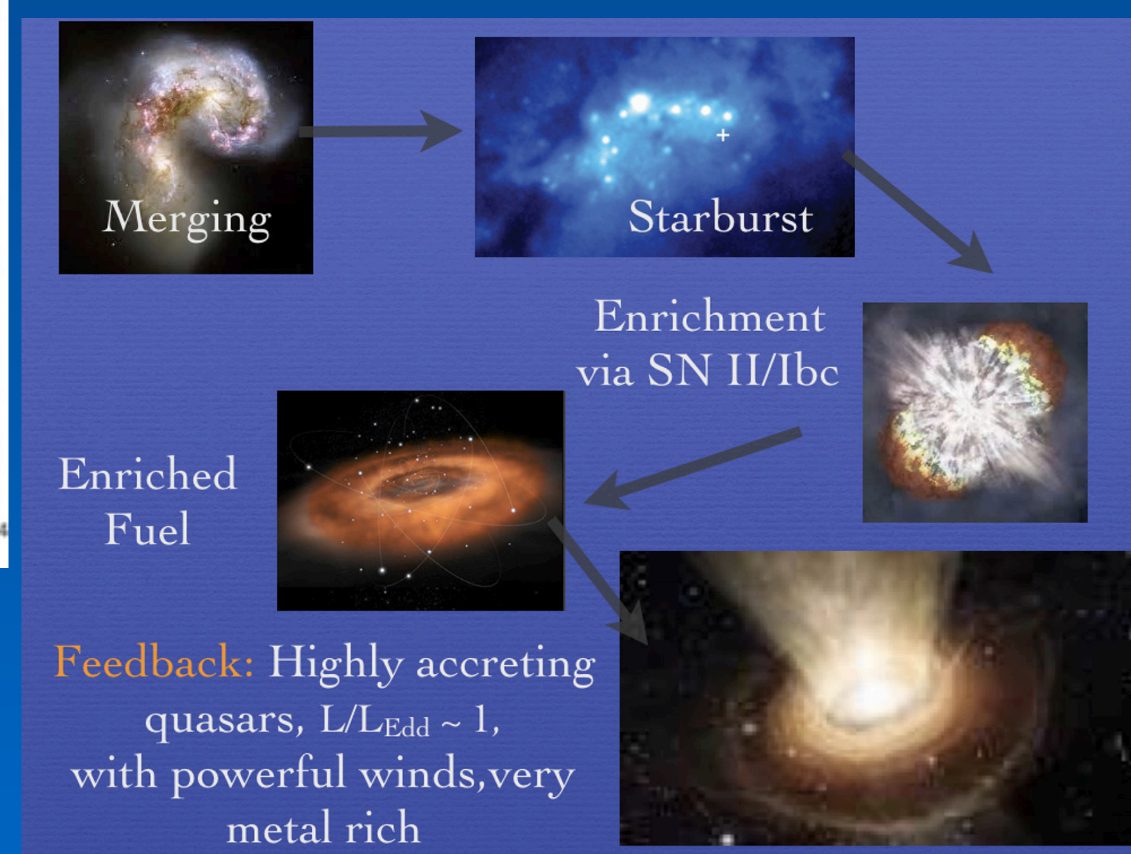

Extreme Population A ($R_{\rm Fe} \gtrsim 1$): implications for Cosmology?

xA: Marziani & Sulentic 2014 (MS14); Negrete et al. 2018; Martínez-Aldama et al. 2018; related to "Super-Eddington" accreting massive black holes (SEAMBHs): Wang et al. 2013; 2014; Du et al. 2016; Czerny et al. 2018 for a review; Czerny et al. 2013; Risaliti & Lusso 2015, and La Franca et al. 2014 for alternative methods.

Extreme Population A: “Eddington standard candles”?

xA quasars: Extreme L/L_{Edd} along the MS with small dispersion

Accretion disk theory: low radiative efficiency at high accretion rate;
L/L_{Edd} saturates toward a limiting value

$$L = \eta L_{\mathrm{Edd}} = \mathrm{const}\,\eta M_{\mathrm{BH}}$$

$$\mathrm{L/L_{Edd}} \rightarrow \mathrm{const.}\quad \mathrm{for}\quad \dot{\mathrm{m}} \gg 1$$

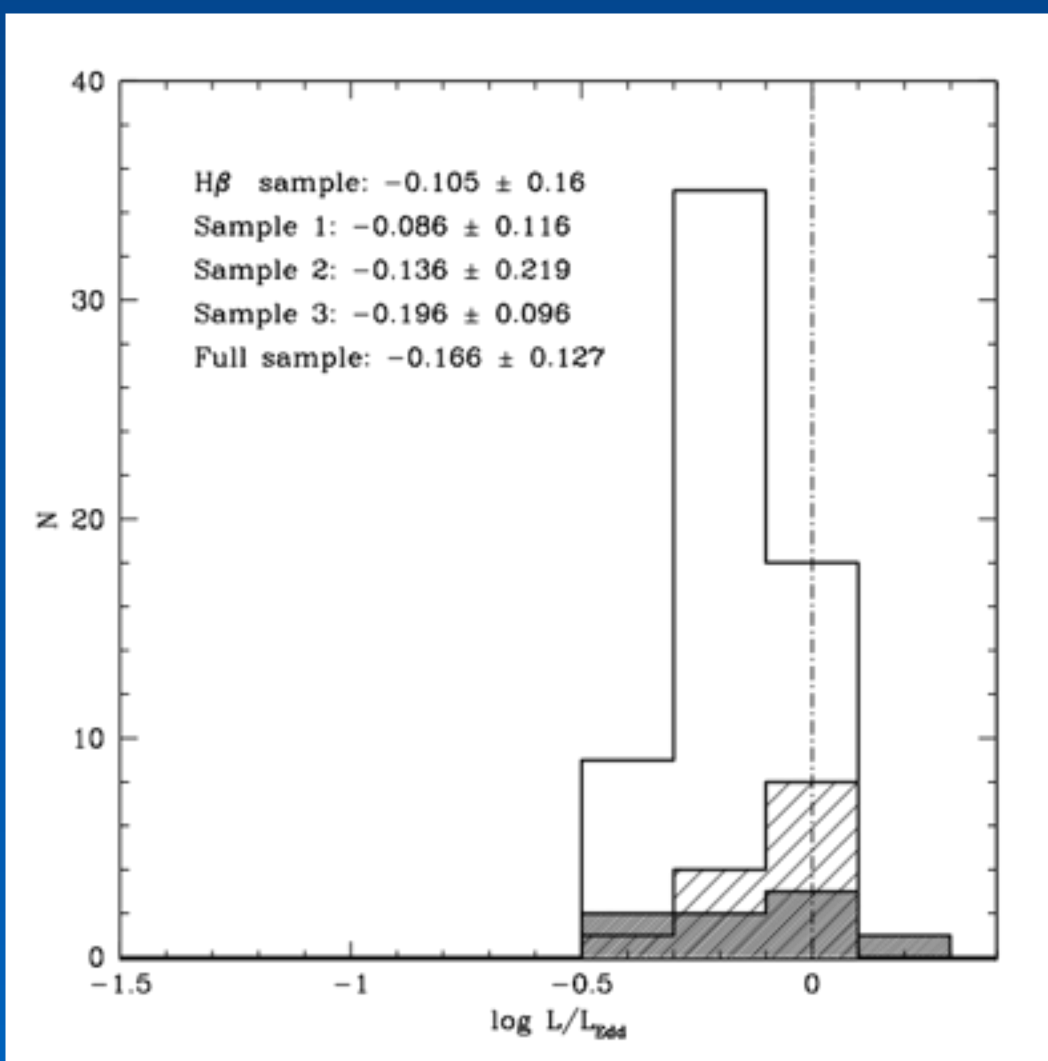

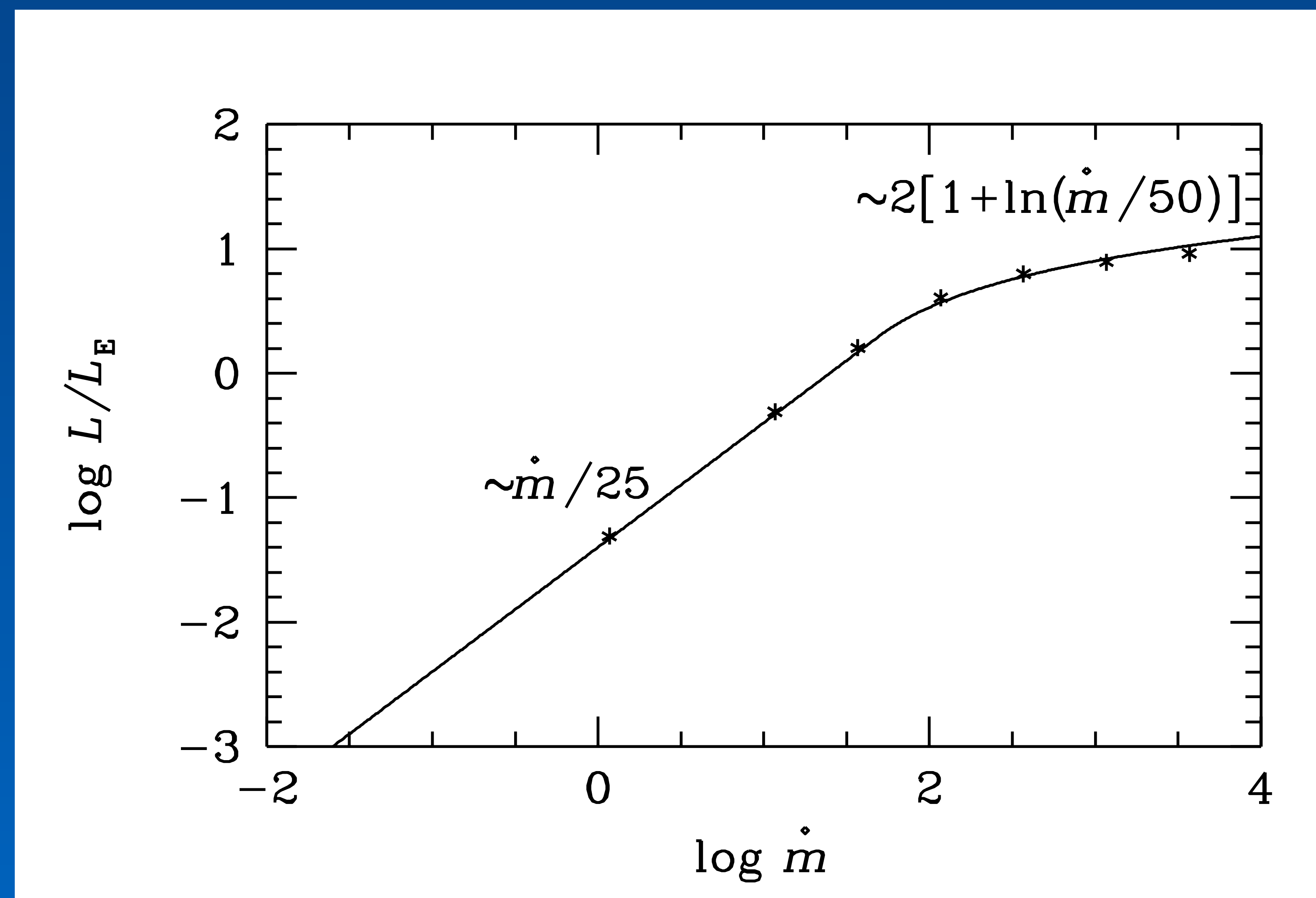

Marziani & Sulentic 2014 (MS14); Mineshige 2000; Abramowicz et al. 1988; Sadowski 2014

Extreme Population A: “Eddington standard candles”?

Eddington standard candles

1. xA quasars radiate close to Eddington limit η~1

$$L = \eta L_{\rm Edd} = {\rm const} \eta M_{\rm BH}$$

2. Assuming virial motions of the low-ion. BLR, L ∝ η M_{BH} ∝ η r_{BLR} $(\delta v)^2$

3. xA quasars have similar BLR physical parameters (n_H and U), implying that the BLR radius rigorously scales as $r_{BLR} \propto [L/(n_H U)]^{1/2}$

geometry
dynamics

$$M_{\rm BH} = \frac{f r (\delta v)^2}{G}$$

r_{BLR}

FWHM
σ,FWZI

fraction of ionizing luminosity

$$L \approx 7.8\ 10^{44} \frac{\eta_1^2 \kappa_{0.5} f_2^2}{\bar{\nu}_{i2.42\ 10^{16}}} \frac{1}{(nU)_{9.6}} \delta v_{1000}^4 \quad {\rm erg\ s^{-1}}$$

average frequency of ionizing photons

“Virial Luminosity:” Analogous to the Tully-Fisher and the early formulation of the Faber Jackson laws for early-type galaxies

MS14; cf. Teerikorpi 2011

Extreme Population A: “Eddington standard candles”?

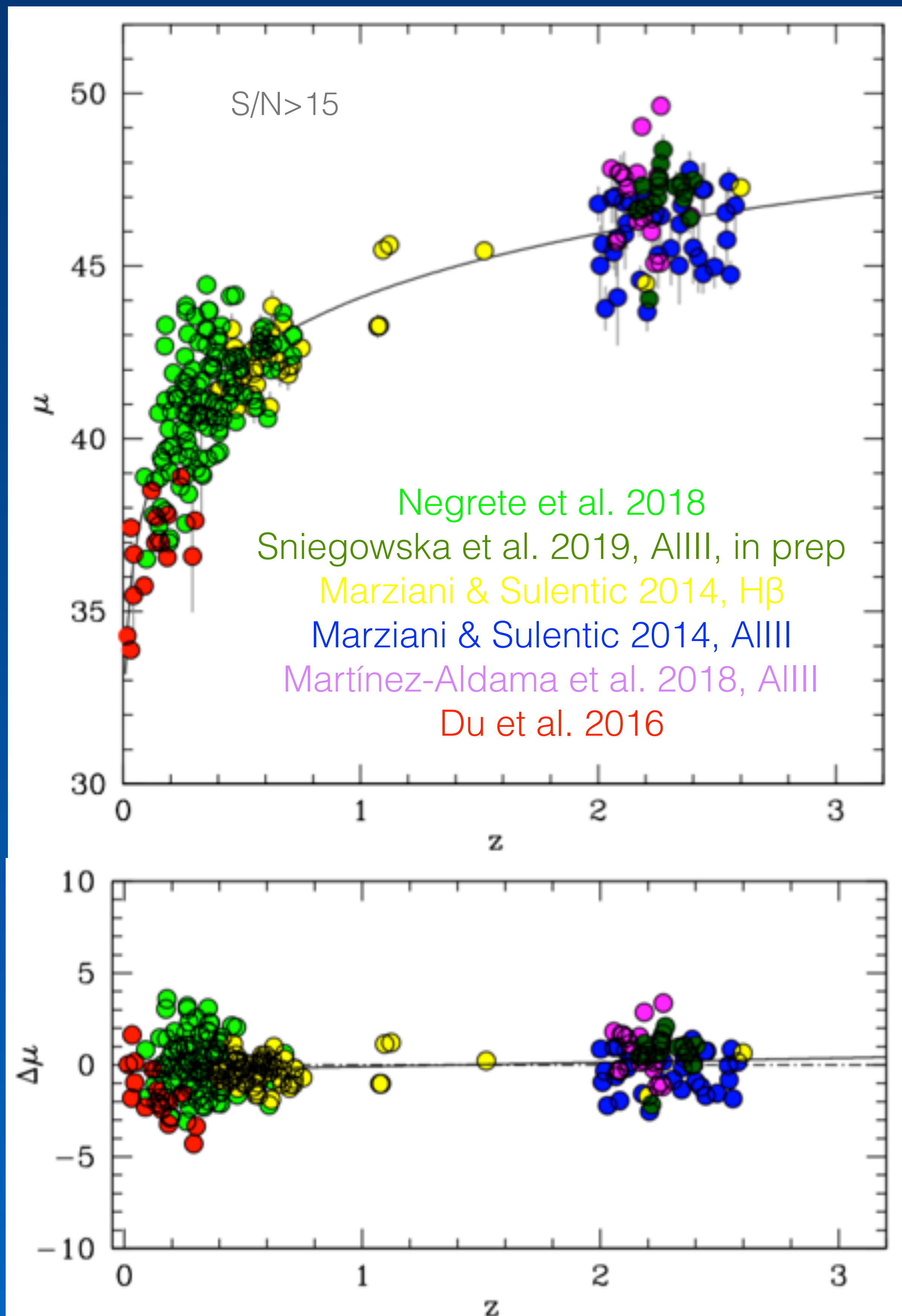

A Hubble Diagram for quasars: consistent with concordance ΛCDM

Significant scatter, $\sigma_{\Delta\mu} \sim 1.1 - 1.3$ mag

Work in progress: data already provide significant constraints on Ω_M (0.30±0.06), better than supernovae, because of the z~2 coverage

Work in progress to reduce the scatter via higher S/N data and an analysis of the main factors affecting the virial broadening estimators

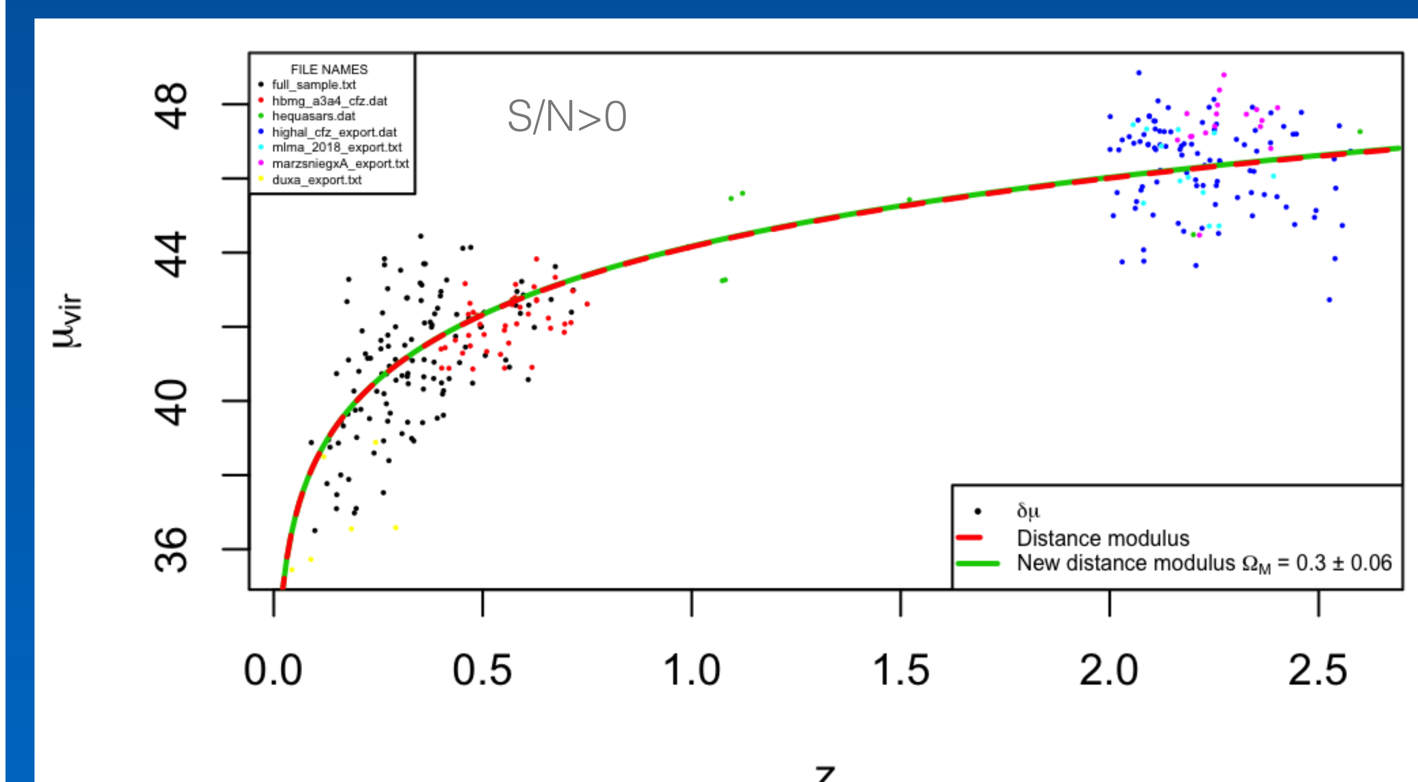

Conclusion

The MS offer contextualization of quasar observational and physical properties.
Several MS trends are associated with relative prominence of outflows, and ultimately with Eddington ratio “convolved with the effect of orientation.”

The differences between Population A and B (“wind-“ and “disk-dominated,” respectively) might be associated with a change of accretion mode (from geometrically thin, optically thick to slim disk?), as several properties appear to change at
$L/L_{Edd} \sim 0.1 - 0.2$.

Extreme Population A (xA) quasars at the high R_{FeII} end of the MS appear to radiate at extreme L/L_{Edd}. xA quasars show a relatively high prevalence (10%) and are easily recognizable. Low ionization lines are apparently emitted in a highly-flattened, virialized BLR.

xA quasars might be suitable as “Eddington standard candles”.

Quasars as distance indicators for cosmology

Sources	Parameters	Basic equation	Reference	Virial
extremely accreting quasars (xA)	Hard X-ray slope, velocity dispersion	$\mathcal{D}_\bullet = \frac{1}{\sqrt{4\pi}}\left[\frac{l_0(1+a\ln\dot{m}_{15})f_{\rm BLR}R_0}{G\kappa_{\rm B}}\right]^{1/2(1-\alpha)}\frac{V_{\rm FWHM}^{1/(1-\alpha)}}{F_{5100}^{1/2}}$	Wang et al.2013	V
extremely accreting quasars (xA)	virial velocity dispersion: FWHM(Hβ) Eddington ratio = const	$L \propto \mathrm{FWHM(H\beta)}^4$	Marziani & Sulentic 2014	V
general quasar populations	X-ray variability, velocity dispersion	$\log\frac{L}{\rm erg\,s^{-1}} + 4\log\frac{\rm FWHM}{10^3\,\rm km\,s^{-1}} = \alpha\log\sigma^2_{\rm rms}+\beta,$	La Franca et al. 2014	V
mainly quasars at z<1	Reverberation mapping time delay τ	$\tau/\sqrt{F} \propto d_L$	Watson et al 2011, 2013; Czerny et al. 2013; Melia 2015	
general quasar populations	non linear relation between soft X and UV	$\log(F_X) = \Phi(F_{UV}, D_L) = \beta' + \gamma\log(F_{UV}) + 2(\gamma-1)\log(D_L),$	Risalti & Lusso 2016	

Eddington standard candles

Data already rule out extreme Universes (Ω_Λ=1,Ω_M=0) or the Einstein-de Sitter Universe

MS14 data already provided significant constraints on Ω_M ($0.19^{+0.17}_{-0.08}$): the redshift range 2 - 3 is highly sensitive to Ω_M

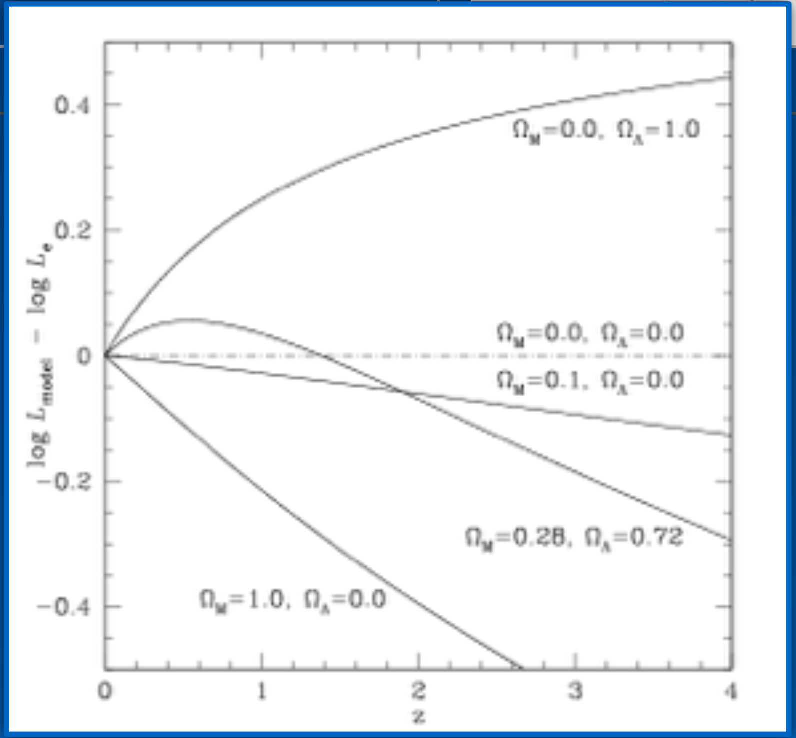

Quasar samples have the potential ability to better constrain Ω_M than supernovae

Samples extending up to z~5 could address the issue of the equation of state of dark energy

Marziani & Sulentic 2014a